AN ABSTRACT OF THE THESIS OF

ANTON POLENSEK (Name) for the DOCTOR OF PHILOSOPHY (Degree)

in CIVIL ENGINEERING (Major) presented on June 1, 1972 (Date)

Title: STATIC AND DYNAMIC ANALYSIS OF WOOD-JOIST FLOORS BY THE FINITE ELEMENT METHOD

Redacted for privacy

Abstract approved: _____
H. I. Laursen

The conventional method for structural design of wood-joist floors is over-simplified and often results in stronger and stiffer floors than necessary. There is also a need to include in the floor design additional criteria dealing with human response to floor vibration such as that due to walking.

This study develops a finite element method for static and dynamic analysis of joist floors. The finite element floor model consists of orthotropic plate elements and composite T-beam elements. The stiffness, mass, damping and load matrices of plate and beam elements are developed using fourth order Hermitian polynomials as displacement functions. Matrix displacement analysis is used to determine the floor response to static loads and numerical integration of equations of motion is used to evaluate the response to dynamic loads. The plate element matrices are verified by analyzing plates

with known solutions and comparing the results. The method applied to floor systems is verified by comparing the analytical results to experimental results from a past study.

Listings of the computer programs developed are included. The programs allow various options as the the type of analysis, structure and loading.

Static and Dynamic Analysis of Wood-Joist Floors By the Finite Element Method

by

Anton Polensek

A THESIS

submitted to

Oregon State University

in partial fulfillment of
the requirements for the
degree of

Doctor of Philosophy

June 1973

APPROVED:

Redacted for privacy

Professor of Civil Engineering

in charge of major

Redacted for privacy

Head of Department of Civil Engineering

Redacted for privacy

Dean of Graduate School

Date thesis is presented June 1, 1972

Typed by Clover Redfern for Anton Polensek

ACKNOWLEDGMENT

The author expresses his appreciation to the Civil Engineering Faculty at Oregon State University for their important influence over the past several years. Special gratitude goes to Dr. Harold I. Laursen for his guidance and encouragement during the formation of this thesis.

The initial stage of this investigation was financially supported in part by the Oregon State University Computer Center, which is acknowledged with appreciation. The investigation has since become a part of a research project on structural performance of wood-joist floors in the Forest Research Laboratory, Oregon State University.

TABLE OF CONTENTS

LIST OF TABLES

LIST OF FIGURES

STATIC AND DYNAMIC ANALYSIS OF WOOD-JOIST FLOORS BY THE FINITE ELEMENT METHOD

I. INTRODUCTION

A wood-joist floor is a complex indeterminate structure consisting of joists and floor covering. It can be compared to an orthotropic plate-membrane reinforced by a set of equidistant ribs. Usually a plywood subfloor attached to joists is the basic component of the plate-membrane, although plywood underlayment, particle board or hardwood flooring, attached to the subfloor, contribute additional stiffness and strength. Wood-joists of various stiffnesses and strengths comprise the ribs. Connections between joists and plywood are either glued, allowing full transfer of shear forces, or nailed, resulting in a partial transfer of shear forces accompanied by the joist-subfloor interlayer slip.

Static analysis involves determination of stresses and deflections under working loads as well as determination of ultimate load for known physical and geometric properties of floor components. Similarly, dynamic analysis deals with dynamic responses, such as frequencies and displacements and responses to walking, impact and other loads that vary with time.

1.1. Justification

Current design practice is based on the assumption that a set of individually acting identical beams can predict highly complex behavior of the joist floor. Therefore, only a single joist acting as a beam needs to be analyzed. This simplification often results in stronger and stiffer floors than necessary and especially penalizes lower grades of lumber. For instance, if designed for a concentrated load, only one joist is assumed to carry this load, even though simple reasoning suggests that in the actual floor a part of the load is transferred to the adjacent joists.

Building codes limit the stresses and deflections of a beam representing the floor to prescribed allowable values (11). The allowable stress for a grade and species of joists is based on their statistical probability distribution of the ultimate stresses. The stress value at the 5% point on the lower side of this distribution is divided by the factor of safety to obtain the allowable stress (2). The span to deflection ratio of 360, usually given by building codes as a deflection limitation, has been used by engineers for nearly a century, but little is known about its origin (19). Reasons, such as plaster cracking in floor-ceiling systems and excessive floor vibrations have been suggested as a basis for deflection limitation (19). Plaster cracking is not much of a problem in present construction, but human response to

floor vibrations caused by walking and impact have received growing attention in recent years (17, 19).

Load distribution across the floor span reduces the stresses in the most flexible joist in the floor. Since there is a direct correlation between the strength and stiffness and since the allowable stress is derived on the basis of a few weaker joists within the grade, the weakest joists in the floor are stressed less than predicted by single beam analysis. A more precise method of static analysis than the existing one, considering the stress distribution across the floor and composite action between joists and subfloor, can only improve the floor design. Past studies have shown that human response to floor vibration can be measured and related to the vibration frequency, amplitude and duration (17). A method of dynamic response analysis can determine these parameters, which can then be used to measure floors with respect to human response to vibration.

1.2. Problem

Two partial differential equations of fourth order, reflecting vertical and membrane displacements, are necessary to describe static behavior of the joist floor. Classical solutions of these equations, perhaps in the form of Fourier series, are limited to certain boundary conditions. Numerical solutions using finite differences require a new solution as soon as the boundary conditions change.

Similar solutions for dynamic analysis may even be impossible to find because of the added effects of inertia and damping forces. The finite element method, which has been chosen in this study, offers more general results. The method not only can be used for various boundary conditions, but also accounts for variations in the stiffness, mass and damping. Dynamic response analysis can be performed without much difficulty by numerical integration of equations of motion, in which the stiffness, mass and damping matrices are formed by combining appropriate matrices for finite elements.

The basic concept of the finite element method consists of representing a structural system as an assembly of a discrete number of elements, generating a stiffness, mass and damping matrix for each element, and finally combining the element matrices into a stiffness, mass and damping matrix of the whole system. The accuracy of the method depends on the type of functions used to describe the displacement of the finite elements. To insure monotonic convergence, i.e., the convergence of the results toward the true solution as the number of finite elements is increased, the displacement functions must meet the following conditions (5):

1) All possible rigid body displacements must be included.
2) All uniform strain states must also be included.
3) Conditions of compatibility must be satisfied not only at the nodal points, but also along all element boundaries and

within the elements.

All these conditions can be satisfied if Hermite interpolation polynomials are used. The application of the fourth, sixth and eighth order Hermite polynomials produced the results that displayed monotonic convergence (16). Naturally, the rate of convergence accelerates as the order of the polynomials becomes larger, but accurate results have been achieved with the fourth order. Polynomials of high order generate element matrices of higher sizes than the polynomials of low order, but the choice of order is somewhat arbitrary. It is not yet known whether it is more efficient to use more low order elements or fewer high order elements (16).

Plywood has been considered as a classical case of an orthotropic material, having three planes of symmetry with respect to its elastic properties. Dong, Pister and Taylor applied the Kirchoff plate bending theory to multilayered orthotropic plates (7). Their stress-strain relationships expressed in matrix form are used in the formulation of the plate element stiffness matrix in this study. In 1943, Newmark developed a theoretical method for a composite T-beam with the slip in the flange-web interlayer (20). The method was first used to analyze concrete slabs with steel beams (20) and later to solve the problem of nailed and glued plywood T-beam panels (1, 13). Wilkinson derived a simple theoretical relationship between the shear load on a nailed joint, a slip corresponding to the shear load,

and the physical and geometric properties of the joint components (25). The contribution of incomplete interaction between joists and subfloor to the stiffness matrix of the wood-joist floor analyzed in this investigation is derived from these studies.

The most important source of damping in a vibrating floor is energy loss due to friction between joists and subfloor, as well as between the subfloor and added flooring. This kind of damping depends on the amount of the interlayer slip that occurs during vibration and has been investigated by Yeh, Hartz and Brown (26). Internal material damping of wood has also been established (12). In addition to slip friction and material damping, other sources of damping are also present in wood-joist floors, such as interlayer friction due to vibration waves across the span, friction between the edges of the adjacent plywood sheets, and the support friction.

1.3 Objective

The objective of this investigation is to develop and verify a theoretical procedure and a computer program for static and dynamic analysis of wood-joist floors. In subsequent studies, the method will be used to investigate more economical spans of wood-joist floors currently being used in housing.

II. FINITE ELEMENT MODEL

This chapter is concerned with the development of the stiffness, mass and damping matrices of the plate and beam elements as well as the load vector for the uniform load acting over the entire area of the plate element.

The model representing the joist floor consists of an assembly of rectangular two-dimensional plate elements and single dimensional beam elements connected at nodal points. The bending and membrane stresses resisted by plate elements are coupled. Similarly, coupling also exists between the bending and axial stresses resisted by beam elements. Stiffness matrices for the plate bending, the beam bending, and the combined effect of the plate membrane and beam axial action can be developed individually and superimposed when the system stiffness matrix is assembled. Each of these three contributions to overall stiffness can be better understood by picturing the floor with no composite action during the deflection. In such a floor, no shear is transferred between the joists and subfloor, and the stiffness is that of the uncoupled plate and beam bending. The corresponding beam element matrices are given by Pestel (16). Plate element matrices are developed in this chapter. In the deflected floor with no composite action, shear forces are next applied to the interfaces of the joists and subfloor until the slip is fully recovered, resulting in a case of

full composite action. The corresponding contribution to the stiffness is also analyzed in this chapter. Finally, partial slip is allowed to develop in the joist-subfloor interlayer, resulting in the stiffness reduction. Past studies provide adequate information to evaluate this reduction due to various nailing patterns (13, 25).

2.1. Properties of Orthotropic Plate Elements

In this development, the plate element is assumed to be plywood which is the most common material for subfloor. However, other materials that sometimes constitute the floor covering can be treated in a similar manner. Structural plywood is usually made of a combination of an odd number of layers of rotary cut wood veneer, rigidly glued together with the grain direction of adjacent plies at right angles. Each layer has a strong direction associated with the longitudinal axis of the wood and a weak direction associated with the radial axis of the wood (23). Assuming that stresses on the planes parallel to the middle surface of the plate are equal to zero, the stress-strain relationship for any layer of an orthotropic plate is (7)

$$\begin{Bmatrix} \sigma_x \\ \sigma_y \\ \tau_{xy} \end{Bmatrix} = \frac{1}{1-\nu_{xy}\nu_{yx}} \begin{bmatrix} E_x & E_x\nu_{yx} & 0 \\ E_y\nu_{xy} & E_y & 0 \\ 0 & 0 & (1-\nu_{xy}\nu_{yx})G_{xy} \end{bmatrix} \begin{Bmatrix} \epsilon_x \\ \epsilon_y \\ \gamma_{xy} \end{Bmatrix} \quad (2.1)$$

where

σ - normal stress

τ - shear stress

E - modulus of elasticity

G - shear modulus

x, y - Cartesian coordinates; as single subscripts they denote the direction of strains and/or stresses

ν_{xy} - Poisson's ratio defining strain in y-direction due to stress in x-direction

Equation (2.1) written in general form is

$$\{\sigma\} = [\bar{C}]\{\epsilon\} \tag{2.2}$$

Since the effect of the coupling between the bending and membrane forces is accounted for later in the development, only plate bending is considered here. The plywood is usually symmetrical with respect to the middle surface, which greatly simplifies the expressions for bending moments. A convenient form for the bending moments, given by Dong et al. (7), can be even further simplified by eliminating terms with membrane stresses. The simplified equation is

$$\begin{Bmatrix} M_x \\ M_y \\ M_{xy} \end{Bmatrix} = - \begin{bmatrix} D_{11} & D_{12} & D_{13} \\ D_{21} & D_{22} & D_{23} \\ D_{31} & D_{32} & D_{33} \end{bmatrix} \begin{Bmatrix} w_{xx} \\ w_{yy} \\ 2w_{xy} \end{Bmatrix} \tag{2.3}$$

where

x, y - Cartesian coordinates; as subscripts they denote partial derivation

w - displacements perpendicularly to x, y-plane

$$D_{ij} = \frac{1}{3} \sum_{k=1}^{n} C_{ij}^{(k)} (h_k^3 - h_{k-1}^3) \tag{2.4}$$

where

$C_{ij}^{(k)}$ - elements of $[\overline{C}]$ in Equation (2.2)

h_k - distance between the middle surface and the top of layer k

h_{k-1} - distance between the middle surface and the bottom of layer k

If either the x or y axis is parallel or perpendicular to the grain direction of the plies no coupling exists between the bending and twisting moments and

$$D_{13} = D_{23} = 0 \tag{2.5}$$

2.2. Stiffness, Mass and Damping Matrix of Orthotropic Plate Elements

The formulation of the element matrices will be performed with the help of Lagrange's equation (3). The first step involves the derivation of the energy for the internal strains, inertia forces and damping forces in terms of displacement functions and their

derivatives. Energy expressions are then substituted into Lagrange's equation and further manipulated to give the desired element matrices.

The rectangular finite element of the orthotropic plate and the nodal displacements are shown in Figure 2. 1a. The internal moments and external load acting on a differential element of the plate are shown in Figure 2. 1b. On the nodal displacements of Figure 2. 1a, the first subscript indicates the nodal point and the subscripts after the comma represent partial derivatives. Symbol w denotes vertical displacements, w_x and w_y are slopes in the x and y directions, respectively, w_{xy} is the change of slope w_x along the y axis and w_{yx} is the change of slope w_y along the x axis. At any point, w_{xy} equals to w_{yx} if the displacement surface is continuous. Nodal forces and moments are positive in the direction of positive nodal displacements.

Strain energy of the plate element is developed next, assuming that the deflection w is small in comparison with the plate thickness and that no membrane forces due to the elongation of the middle surface need to be considered. The development given by Timoshenko and Woinowsky-Krieger for isotropic plates (22) requires only minor adjustments to obtain the strain energy for orthotropic plates. The differential area of the plate and the moments acting on it are shown in Figure 2. 1b. The work done by bending and twisting moments on this differential area is (22)

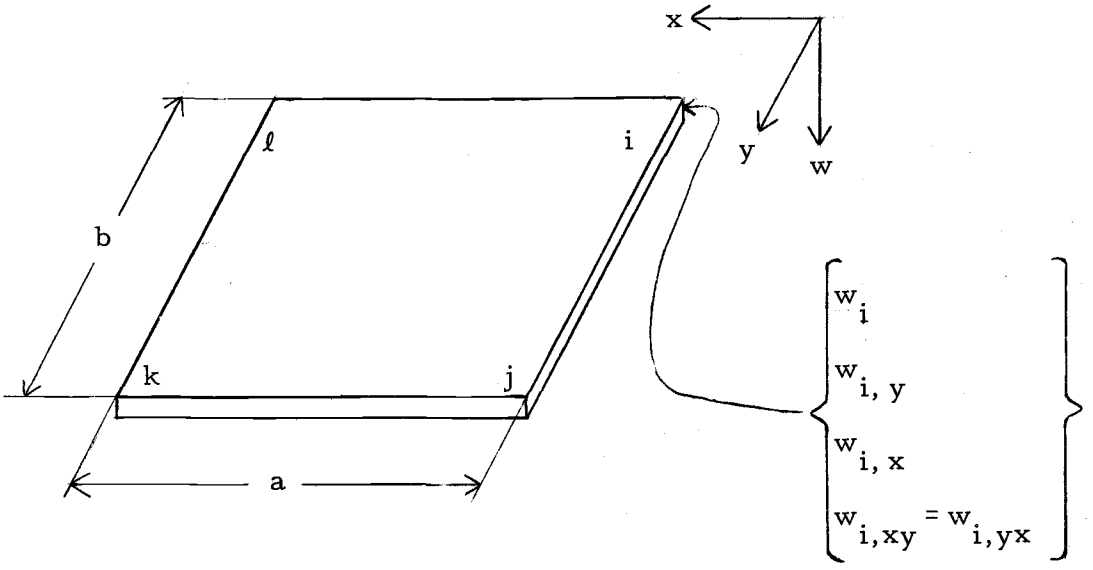

(a) Finite element and nodal displacements.

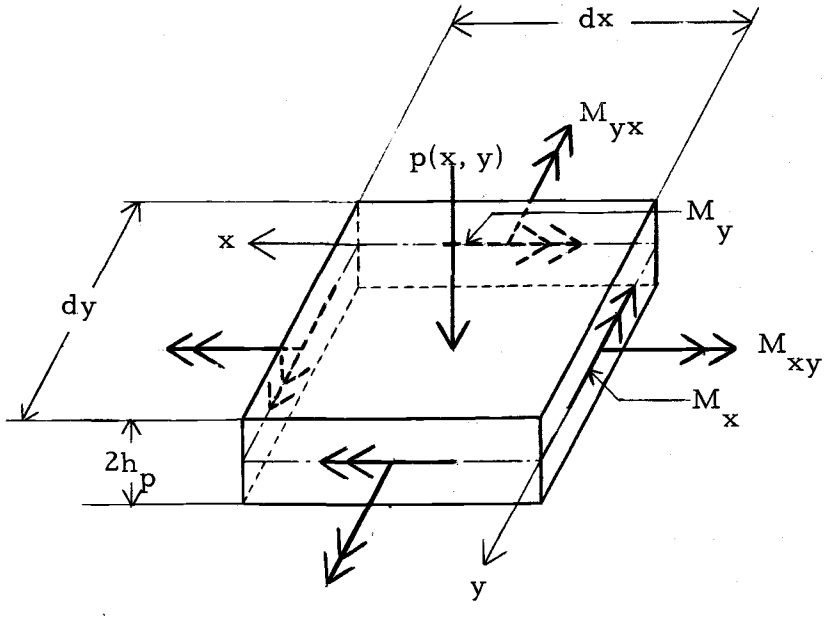

(b) Moments and forces.

Figure 2.1. Bending rectangular plate element.

$$dU = \frac{1}{2}(-M_x w_{xx} - M_y w_{yy} + 2M_{xy} w_{xy})dxdy \tag{2.6}$$

Substituting Equation (2.3) into Equation (2.6) gives the desired energy expression

$$dU = \frac{1}{2}(D_{11} w_{xx}^2 + 2D_{12} w_{xx} w_{yy} + D_{22} w_{yy}^2 + 4D_{33} w_{xy}^2)dxdy \tag{2.7}$$

The kinetic energy of the differential mass dm is

$$dK = \frac{1}{2}\dot{w}^2 dm = \dot{w}^2 \rho h_p dxdy \tag{2.8}$$

where

ρ - plate density

h_p - one-half plate thickness

The dot denotes partial differentiation with respect to time t. For harmonic motion

$$\dot{w}(x, y, t) = w(x, y)\frac{\partial}{\partial t}(e^{i\omega t}) = i\omega w(x, y, t) \tag{2.9}$$

where

ω - circular frequency

The arguments of w will not be shown in subsequent developments.

The potential energy of the differential area due to viscous damping is

$$dW_c = -c\dot{w}w dxdy \tag{2.10}$$

where

$$c = 2\lambda\rho 2h_p\omega_1$$

λ - damping ratio in the lowest mode, in percentage of critical damping

ω_1 - the lowest modal frequency

The negative sign in Equation (2.10) comes from the fact that the positive damping force acts in the direction of negative w. The damping coefficient selected in this investigation is the coefficient associated with the lowest mode of vibration. The lowest mode is usually used if the dynamic response analysis is performed by the numerical integration of equations of motion.

The standard form of Lagrange's equation is (3)

$$\frac{d}{dt}\left(\frac{\partial K}{\partial \dot{g}_m}\right) - \frac{\partial K}{\partial g_m} + \frac{\partial U}{\partial g_m} - \frac{\partial W_c}{\partial g_m} = \frac{\partial W_e}{\partial g_m} \qquad (2.11)$$

where

g_m - generalized coordinates

W_e - work done by external forces

Integrating Equations (2.7), (2.8) and (2.10) over the entire element area, substituting the results into Equation (2.11), and rearranging terms results in the equations of motion

$$-\omega^2 \int_0^a \int_0^b 2\rho h_p \, w \frac{\partial w}{\partial g_m} \, dxdy + \int_0^a \int_0^b \Bigg[D_{11} w_{xx} \frac{\partial w_{xx}}{\partial g_m}$$

$$+ D_{12} \left(w_{yy} \frac{\partial w_{xx}}{\partial g_m} + w_{xx} \frac{\partial w_{yy}}{\partial g_m} \right) + D_{22} \, w_{yy} \frac{\partial w_{yy}}{\partial g_m} + 4D_{33} \, w_{xy} \frac{\partial w_{xy}}{\partial g_m} \Bigg] dxdy$$

$$+ i\omega \int_0^a \int_0^b cw \frac{\partial w}{\partial g_m} \, dxdy = \int_0^a \int_0^b \frac{\partial W_e}{\partial g_m} \, dxdy \qquad (2.12)$$

As suggested by Pestel (16), displacement functions w can be expressed in terms of Hermitian polynomials and nodal displacements. The procedure is carried out for the fourth order polynomials in Appendix A.

The general form of the equations of motion expressed in matrix form is (27)

$$(-\omega^2[M] + [K] + i\omega [C]) \{w\} = \{P\} \qquad (2.13)$$

where

[M] - mass matrix

[K] - stiffness matrix

[C] - damping matrix

{w} - displacement vector

{P} - external force vector

Generalized coordinates in Equation (2.12) correspond to the elements of the displacement vector. A partial derivative of Equation (2.12)

with respect to the first element of the displacement vector gives the first row of the element matrices. Derivatives with respect to successive elements give the remaining rows. Comparing Equation (2.12) to Equation (2.13) suggests that the first double integral on the left side of Equation (2.12) belongs to the mass matrix, while the second and the third one belong to the stiffness and damping matrices, respectively.

Since the density, thickness and material damping are constant throughout the floor covering, quantities ρ, h_p, and c in Equation (2.12) are exempted from integration. The remaining variables in the first and the third integral of Equation (2.12) are the same, making both integrals identical. Therefore, the damping matrix can be expressed in terms of the mass matrix

$$[C] = \lambda\omega_1[M] \tag{2.14}$$

The partial differentiation and integration of Equation (2.12) is performed in Appendix A. The final form of the stiffness matrix is

$$[K] = \frac{1}{30ab}\lceil L\rfloor\left(\frac{p^{-2}}{7}D_{11}[K_1]+\frac{1}{15}D_{12}[K_2]+\frac{p^{2}}{7}D_{22}[K_3]+\frac{2}{15}D_{33}[K_4]\right)\lceil L\rfloor \tag{2.15}$$

where

$$p = \frac{a^2}{b^2}$$

$\lceil L\rfloor$ - defined by Equation (A.25)

$[K_1]$ - defined by Equation (A.27)

$[K_2]$ - defined by Equation (A.28)

$[K_3]$ - defined by Equation (A.29)

$[K_4]$ - defined by Equation (A.30)

The displacement vector $\{w\}$ is defined by Equation (A.14). The mass matrix is

$$[M] = \frac{abph_p}{176400} [L][\overline{M}][L] \tag{2.16}$$

where $[\overline{M}]$ is defined by Equation (A.31)

2.3. Properties of the Composite T-Beam Element

Properties of the composite T-beam element can be visualized as a combination of the plate, joist and connection properties. Plate properties were discussed in Section 2.1. The joist properties vary greatly within each lumber grade and species. A 2 to 1 ratio between the maximum and the minimum value of the modulus of elasticity is quite common. The mass density and moment of inertia are more uniform, but they are far from being the same for each joist. Simple measurement and weighing can be used to establish the moment of inertia and mass of joists. A standard test specified by the American Society for Testing and Materials is used to evaluate the modulus of elasticity (2). A damping ratio of 0.35% of critical damping is usually

taken for the material damping in wood construction (12).

The evaluation of the connection properties is somewhat more complex. A rigid glue assures full composite action, but it is seldom used because it requires controlled gluing operations. Although recently introduced semi-rigid elastomeric adhesives have been used extensively for floor gluing (18), nails are still the most common means of the joist-subfloor connection. Therefore, the most common types of wood-joist floors are those with incomplete interaction accompanied by the interlayer slip. The mechanism of the shear transfer through the nailed connection cannot be described by a simple linear load-deflection relationship, but by a more complex non-linear behavior. Yeh studied this mechanism on nailed double shear specimens by observing the relationship between the static cyclic load and the relative displacement, i.e., slip, between the connected elements (26). A typical diagram and the specimen are shown in Figure 2.2. During the initial cycle, the load was transferred by static friction up to 20 lbs, at which point slip occurred. As the load was increased to 80 lbs the slip progressed and the nails transferred more and more load. Only about 12% of the slip was recovered when the load was reduced to 5 lbs. Nine additional load cycles produced a significant increase in the slip, but only negligible slip occurred during the next 90 cycles. Since the load on the specimen was never reversed, a minimum bearing pressure due to frictional forces between the joined

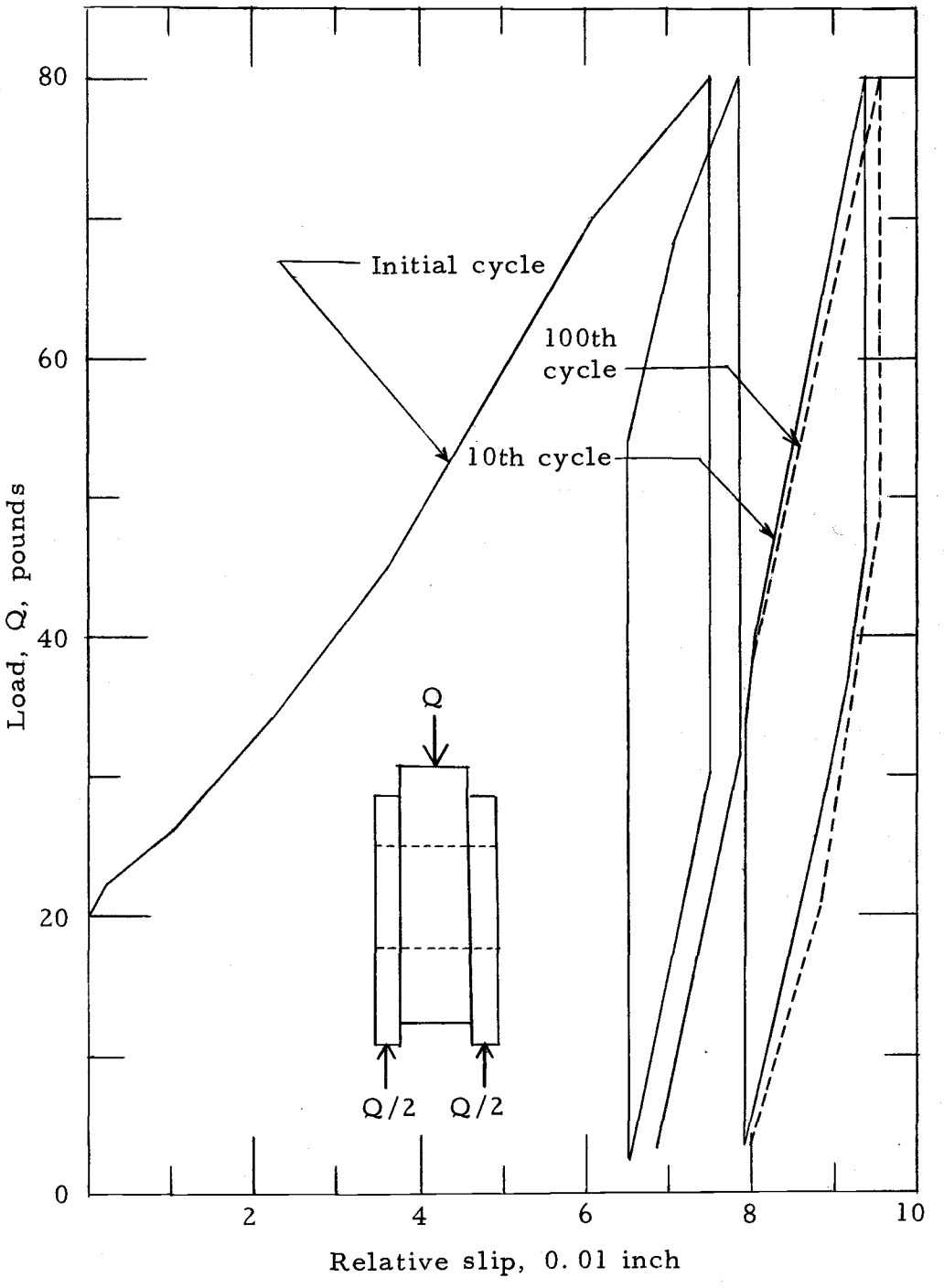

Figure 2.2. Cyclic load diagram of nailed shear specimen.

pieces of wood acted on the nails even after the load Q was removed from the specimen. Therefore, the relative displacement between the connected pieces of wood became permanent and the shear transfer through the interlayers followed bi-linear elastic behavior (Figure 2.2). This mechanism of shear transfer closely resembles that of a nailed wood joist floor under static load. After some time in service, the slip associated with the nail bearing becomes orderly and Kuenzi's theoretical model and solution for lateral nail bearing applies (13). The core of this model is the assumption that nailed joints subjected to lateral loads behave like beams on an elastic foundation in which the nails are beams and the wood represents an elastic foundation. The pressure under the nail is assumed to be proportional to the nail deflection and no shear is transferred by friction between the joined pieces of wood.

The modulus of the shear connector, used to define shear joints (20), is given by

$$k = \frac{\gamma}{Q} \tag{2.17}$$

where

γ - relative slip between the connected elements

Q - load on the connector

Using Kuenzi's solution, Wilkinson gives graphs (25), by which the modulus k for the nailed joint with one nail can be found, once the

properties of the nail and connected elements are known. Since the subfloor is usually nailed to joists with equally spaced nails of equal capacities, the shear modulus for subfloor-joist connections is expressed per unit length, i.e., the value according to Wilkinson is divided by the nail spacing.

Damping due to the energy loss caused by the slip friction in the subfloor-joist interlayer is the major source of damping in wood-joist floors. Yeh et al., studied the mechanism of slip damping in nailed joist-plywood T-beams (26). They established the relationship between the damping ratio and the beam midspan deflection for various values of the shear connector modulus. The damping greatly depends on the amount of the slip present. During the beam deflection, the damping ratio at the time of the maximum slip and no nail bearing is about ten times larger than at the time of the minimum slip and the full nail bearing (Figure 2.2).

The use of a constant shear connector modulus should give sufficient accuracy if static analysis is performed, but may fail to produce accurate results in the case of dynamic response analysis. The variation of the shear connector modulus and the damping ratio with respect to the floor deflection has not been a subject of this study, but it can be incorporated into the dynamic response analysis when additional empirical information becomes available.

2.4. Stiffness, Mass and Damping Matrix of the Composite T-Beam Element

The coupling between the bending and membrane forces in the floor covering and the coupling between the bending and the axial forces in joists present considerable difficulty in finding the exact solution. The interlayer slip complicates the solution even further. Instead of trying to find the exact solution to this problem, past studies which offer a rather accurate approximate solution are applied. Amana and Booth solved this problem for a single T-beam, visualizing the floor as a set of identical T-beams (1). Their tables are used in this study to estimate the effective width of the T-beam for complete composite action to determine the contribution of this action to the composite beam stiffness matrix. The effect of the slip is accounted for by using stiffness reduction factors given by Kuenzi and Wilkinson (13).

The stiffness of the composite T-beam element is evaluated next. The forces acting on the cross-section of the element are shown in Figure 2.3. Forces N_p and N_b, of the same magnitudes but opposite direction, are applied at the interlayer to the plate and joist, respectively, to restore the compatibility between the plate and joist. Both N_p and N_b are then transferred to the middle surface and neutral axis, respectively, as indicated in Figure 2.3. The moments resisting external forces are M_p for the plate bending and M_b for

the beam bending.

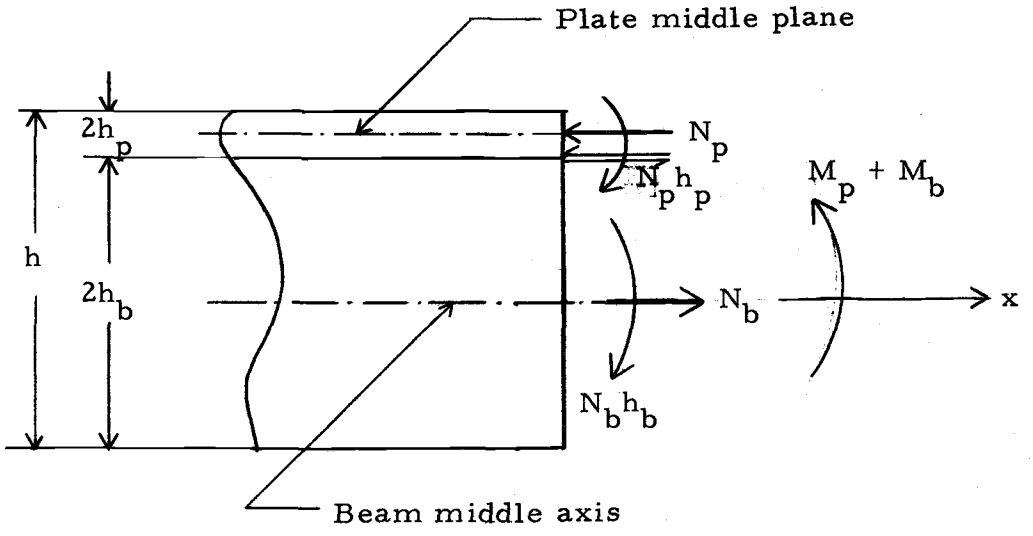

Figure 2.3. Forces on the composite beam element.

The slip γ in the interface is

$$\frac{d\gamma}{dx} = \epsilon_b - \epsilon_p \tag{2.18}$$

where

$$\epsilon_b = u_{b,x} - t_b(w_{b,xx} - \bar{w}_{b,xx}) \tag{2.19}$$

$$\epsilon_p = -u_{p,x} + t_p(w_{p,xx} - \bar{w}_{p,xx}) \tag{2.20}$$

ϵ - strains at the beam-plate interface

b - subscript denoting beam

p - subscript denoting plate

u - axial and/or membrane deformation at interface

w - deflection for no interaction

$\bar{w}$ - deflection recovery due to interaction

The evaluation of strains in the beam presents no difficulty, but the strains in the plate cannot be found unless their distribution in the direction across the span is known.

The distribution of membrane strains and forces in the floor covering is not uniform, but follows a more complicated pattern with a peak at each joist in the form known as shear lag (Figure 2.4). The actual force distribution can be replaced by an equivalent uniform distribution of the width b_e, which is referred to as effective width. If each joist, attached to the plate of the width b_e to form a T-beam, is treated individually, the stiffness contribution of the composite action can easily be evaluated. By applying the solution of the single T-beam analysis, the compatibility of membrane displacements is violated at the junction of the adjacent T-beams but the resulting errors are assumed to be tolerable. Sample calculations showed that the effective width greatly depends on the span to joist spacing ratio. This ratio is in most wood joist floors of such magnitude that it completely dominates other factors and the effective width can in most cases be made equal to the joist spacing. The final results of this study support this reasoning.

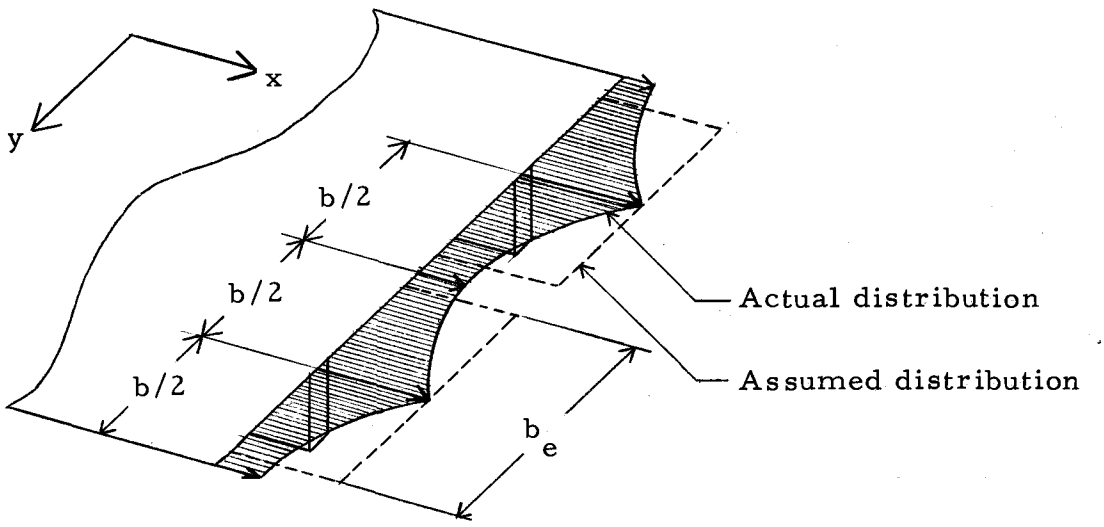

Figure 2.4. Distribution of membrane forces in the floor covering.

In this study the composite beam stiffness is evaluated for the T-beam with a uniform distribution of membrane forces. The basic steps in this development are general enough to be easily applied to the T-beam with an assumed non-uniform distribution of membrane forces. The final result is in somewhat more convenient form than it would be if the conventional T-beam analysis were used.

From the equilibrium condition between N_b and N_p the relationship between the slope of the plate membrane displacements $u_{p,x}$ and the slope of the beam axial displacements $u_{b,x}$ is obtained

$$u_{b,x} = \frac{b_e A_{11}}{A_b E_b} u_{p,x} \tag{2.21}$$

where

$$A_{11} = \sum_{k=1}^{n} C_{ij}^{(k)} (h_k - h_{k-1}) \tag{2.22}$$

A_b - area of joist cross-section

E_b - modulus of elasticity of joist

$C_{ij}^{(k)}, h_k, h_{k-1}$ - defined in Section 2.1

Since vertical displacements of the plate and the beam are equal

$$w_{p,xx} = w_{b,xx} = w_{xx} \tag{2.23}$$

and

$$\overline{w}_{p,xx} = \overline{w}_{b,xx} = \overline{w}_{xx} \tag{2.24}$$

For complete composite action, γ in Equation (2.18) is zero. Substituting Equations (2.21), (2.23) and (2.24) into Equations (2.19) and (2.20) and then substituting the results into Equation (2.18), with γ taken as zero, gives

$$w_{xx} - \overline{w}_{xx} = \frac{2}{h} \left(1 + \frac{b_e A_{11}}{A_b E_b}\right) u_{p,x} \tag{2.25}$$

The total resisting moment of the composite T-beam cross section is

$$M_p + M_b + N_b \frac{h}{2} = -(w_{xx} - \overline{w}_{xx})(EI)_{eff} \tag{2.26}$$

where

$(EI)_{eff}$ - effective stiffness of the cross-section

Conventional expressions relating internal forces and displacements are substituted into the left side of Equation (2.26) to obtain

$$(w_{xx}-\bar{w}_{xx})[(EI)_{eff}-b_e D_{11}-E_b I_b] = hb_e A_{11} u_{p,x} \qquad (2.27)$$

where

I_b - beam moment of inertia

Dividing Equation (2.27) by Equation (2.25) and rearranging terms gives the final expression

$$(EI)_{eff} = b_e D_{11} + E_b I_b + \frac{h^2 b_e A_{11}}{4(1+\frac{b_e A_{11}}{A_b E_b})} \qquad (2.28)$$

Equation (2.28) is equivalent to the stiffness expression derived by the conventional T-beam analysis. The term $b_e E_{11}$ in Equation (2.28) represents the plate bending stiffness in the x-direction and has been included into the plate stiffness matrix in Section 2.2. The term $E_b I_b$ is the beam bending stiffness. The last term on the right side of Equation (2.28) defines the stiffness due to the complete composite action between the beam and plate. This stiffness is visualized as an additional beam stiffness, so that the composite beam stiffness matrix

can be written as

$$[K_b] = \frac{1}{a^3}\left(E_b I_b + \frac{h^2 b_e A_{11}}{4(1+\frac{b_e A_{11}}{A_b E_b})} \right) \lceil L_b \rfloor [\bar{K}_b] \lceil L_b \rfloor \qquad (2.29)$$

where

a - length of the beam element

$\lceil L_b \rfloor$ - defined by Equation (A.32)

$[\bar{K}_b]$ - defined by Equation (A.33)

The development of $[\bar{K}_b]$ using the fourth order Hermitian polynomials and Lagrange's equation is given in Reference 16.

The beam displacement vector is defined by

$$\{w_b\} = \begin{Bmatrix} w_i \\ w_{i,x} \\ w_\ell \\ w_{\ell,x} \end{Bmatrix} \qquad (2.30)$$

The beam finite element, internal moments and nodal displacements are shown in Figure 2.5.

The mass matrix depends on the distribution of the mass and the displacement functions, which are independent of the composite action. Therefore, the composite beam mass matrix is the same as the beam mass matrix given by Pestel for the fourth order Hermitian

polynomials (16). This mass matrix can be written in the following form

$$[M_b] = a\rho_b [L_b][\overline{M}_b][L_b] \tag{2.31}$$

where

ρ_b - beam mass per unit length

$[\overline{M}_b]$ - defined by Equation (A. 34)

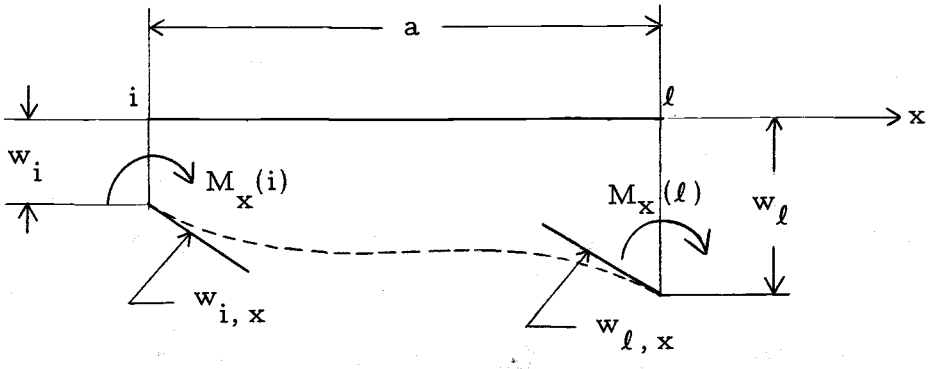

Figure 2.5. Composite T-beam bending element.

Like the plate element damping matrix, the composite beam damping matrix can be expressed in terms of the mass matrix

$$[C_b] = (\lambda_m + \lambda_s)\omega_1 [M_b] \tag{2.32}$$

where

λ_m - damping ratio for material damping

λ_s - damping ratio for slip damping

Both damping ratios, λ_m and λ_s, are assumed to be constant along the beam.

2.5. Load Vectors

If no external forces act on the floor, the right side of Equation (2.13) becomes zero, as the forces along the two adjacent elements cancel out when the finite element matrices are combined into the system matrices. External concentrated loads acting at nodal points need no special evaluation. The loads are simply placed in the appropriate positions in the load vector. However, the load matrix for distributed external loads requires the evaluation of the right side of Equation (2.11). If the function $p(x, y)$ defines an external load, the right side of Equation (2.11) becomes

$$\frac{\partial W_e}{\partial g_m} = Q_m = \int_0^a \int_0^b p(x, y) \frac{\partial w}{\partial g_m} \, dxdy \qquad (2.33)$$

where

Q_m - element of the load matrix corresponding to element g_m of the displacement matrix

Equation (2.33) can be evaluated in the same way as Equation (2.12). For the fourth order Hermitian polynomials and uniformly distributed load p, the load matrix is

$$\{Q\} = \frac{abp}{144} \lceil L \rfloor \{p\} \qquad (2.34)$$

which corresponds to Equation (A.35).

III. METHOD OF ANALYSIS

The assembly of the element matrices into the system matrices, methods of static and dynamic analysis of wood-joist floors, and a brief discussion of dynamic loads acting on residential floors are the topics of this chapter. Because the methods of analysis used are readily available in literature, they are only outlined here and more attention is given to the aspects typical of joist floors.

An assembly of the plate and the composite T-beam elements is shown in Figure 3.1. The composite T-beams of length a offer no resistance to plate bending. Rectangular sections of the floor covering form the plate elements. All of the local coordinate systems are oriented the same and have their origins at nodal point i of each plate element. The plate element sides i-ℓ and j-k are always parallel to the x-axis and the sides i-j and ℓ-k are always parallel to the y-axis. A single plate element usually spans two adjacent joists, i.e., the width b always is the joist spacing except when a concentrated load is applied between the adjacent joists. Composite T-beam elements are placed along the i-ℓ and j-k sides of the plate element so that the beam neutral axis lies in the plate middle surface and the nodal points i and ℓ of the beam correspond to the plate nodal points i and ℓ, and/or j and k.

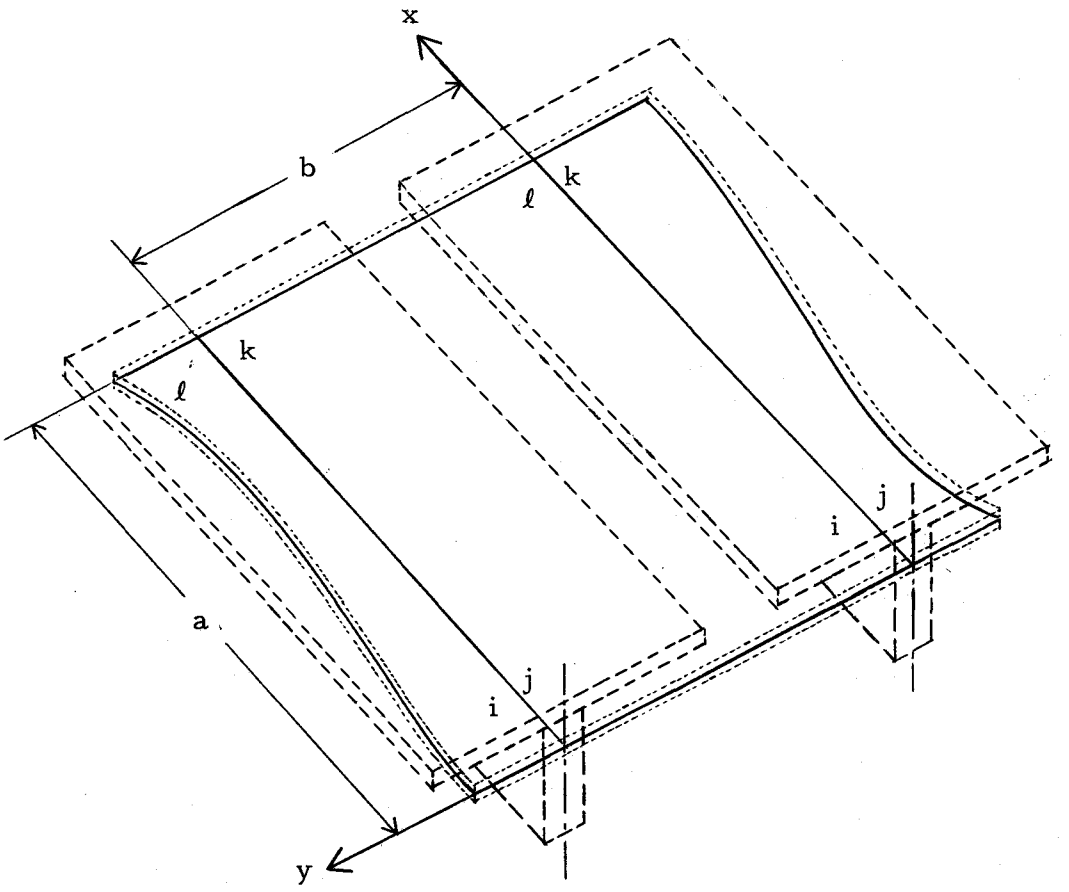

Figure 3.1. The floor model and the assembly of the plate and beam elements.

The plate and beam elements as shown in Figure 3.1 provide the basis for the assembly of the stiffness, mass, damping and force matrix of the floor system, using the element matrices developed in Chapter II. Tezcan's code number procedure (14, 21), used to accomplish the assembly, is particularly efficient in forming banded matrices (14) which can result in a considerable saving of storage space in the computer. The smallest bandwidth is obtained if the

nodal displacements are numbered in an order that produces for each finite element the smallest difference between the largest and the smallest nodal displacement number. In the floor system, this is accomplished by starting the numbering at one floor end and continuing across the span to the opposite end.

Once the system matrices are determined, all of the structural properties of the floor system become defined in a manner suitable for formulation of the three types of conditional equations, the solutions of which give the desired parameters. The first type of equations is associated with static analysis, the second type with frequency analysis and the third type with dynamic response analysis of the joist floor system.

3.1. Static Analysis

As pointed out in Chapter I, maximum deflections and stresses in the joists and subfloor, caused by the uniform and concentrated loads, govern the design of wood-joist floors. These deflections and stresses are a subject of this study. Most floors not only have simple supports with no fixation, but also have simple spans. Since the maximum deflections and stresses of these floors usually appear at the midspan, their finite element mesh is the easiest to establish. Continuous joist floors over several supports and floors with an overhang, often found in larger residential structures, may require a

more complex mesh, but are otherwise analyzed in much the same way as floors with a single span.

Displacements are computed by the matrix displacement method (14). Actually, only the final displacement equation of this method is used. The method is primarily concerned with the development of the system stiffness matrix which has already been determined for the floor system. The term displacement method as used herein refers to the process in which the system displacement vector $\{w_s\}$ is determined by the following equation (14)

$$\{w_s\} = [K_s]^{-1}\{P_s\} \tag{3.1}$$

where

$[K_s]$ - system stiffness matrix

$\{P_s\}$ - system vector of external forces

If the maximum joist deflection is also one of the nodal displacements, the solution is complete. Sometimes the floor system and the loading can be of such a type that the point of maximum joist deflection cannot be predicted in advance and none of the nodal displacements will represent the maximum joist deflection. In this case the displacements along the beam elements can be determined by Equation (A.9) or a new analysis is carried out using a different mesh. In most cases the first solution should be preferable.

Moments and stresses in the joists and floor covering depend on

the nodal displacements and the material properties defined in Chapter II. If no symmetry exists, each of the finite elements meeting at a nodal point undergoes different displacements so that each of them gives different internal nodal moments. The effective nodal moments usually are obtained by averaging the corresponding element values (15, 27). Since the fourth order Hermitian polynomials used as displacement functions result in a linear variation of moments within each element, the moments and stresses can easily be established not only at the nodal points but at any point in the floor.

The conventional moment-curvature relationship is used to determine moments in joists. At the nodal displacement ℓ of the beam element i-ℓ (Figure 2.5), the moment M_x is given by

$$M_x = -(EI)_{eff} w_{\ell, xx} \tag{3.2}$$

where

$(EI)_{eff}$ - defined by Equation (2.28)

The curvature $w_{\ell, xx}$ is given as the value of the second derivative of Equation (A.9) with respect to x at the point ℓ

$$w_{\ell, xx} = \frac{1}{a^2} [6(w_i - w_\ell) + 2a(2w_{\ell, x} + w_{i, x})] \tag{3.3}$$

The moment at the nodal point of a joist is the average value for the two adjacent elements.

The maximum stress σ_x at the point ℓ of the beam element is

$$\sigma_x(\ell) = c_b w_{\ell, xx} E_b \tag{3.4}$$

where

$$c_b = h_b + \frac{h}{2\left(\frac{E_b A_b}{A_{11} b_e} + 1\right)} \tag{3.5}$$

The symbols E_b, h_b, h, A_b, A_{11} and b_e are defined in Chapter II; c_b is the distance between the neutral axis of the composite beam and the bottom of the joist.

The bending moments and stresses in the y direction of the floor covering govern the choice of the thickness of the floor covering and the joist spacing. Because joist stiffnesses vary, these stresses are caused not only by the concentrated loads but also by the uniform load. The moment $M_y(\ell)$ at nodal point ℓ of the plate element i, j, k and ℓ is calculated by Equation (2.3), in which the curvature $w_{\ell, xx}$ is defined by Equation (3.3) and the curvature $w_{\ell, yy}$ is equal to the partial derivative of Equation (A.9) with respect to y at the point ℓ

$$w_{\ell, yy} = \frac{1}{b^2}\left[6(w_k - w_\ell) - 2b(2w_{\ell, y} + w_{k, y})\right] \tag{3.6}$$

In the case of the plywood floor covering the maximum stress $\sigma_y(\ell)$ at the point ℓ of the plate element is obtained from stress-strain-

curvature relationships for the top of the plate $(z = h_p)$

$$\sigma_y(\ell) = \frac{E_x}{1-\nu_{xy}\nu_{yx}} [h_p w_{\ell,yy} + \nu_{yx}(h-c_b) w_{\ell,xx}] \tag{3.7}$$

and/or for the bottom of the plate $(z = -h_p)$

$$\sigma_y(\ell) = \frac{E_x}{1-\nu_{xy}\nu_{yx}} [-h_p w_{\ell,yy} + \nu_{yx}(2h_b - c_b) w_{\ell,xx}] \tag{3.8}$$

where all the terms have been defined earlier in the text. In the computer program, both values of σ_y are computed at each point, but only the maximum value is retained. Effective values of M_y and σ_y at the nodal point are determined by averaging the values for adjacent elements.

A considerable amount of computation can be saved if the floor exhibits some sort of symmetry, because only part of the floor needs to be analyzed if proper displacements are introduced along the symmetry axis. For instance, by taking advantage of symmetry and analyzing only one-half of the structure, the size of the system matrices of a symmetrically loaded, simply supported floor with a single span is reduced to one-half of the size for the complete floor.

3.2. Modal Frequencies

In the finite element system, each elastic degree of freedom is

associated with a natural frequency and corresponding modal shape which is defined by a modal vector if matrix form is used. The evaluation of the natural frequencies and modal vectors, known either as an eigen- or frequency analysis, is a frequent phase of the dynamic analysis of complex structures. Both the frequencies and vectors are required for the modal response analysis, but only a few frequencies need to be known if the dynamic response analysis is performed by numerical integration of the equations of motion (3, 27). In either case, both the frequencies and vectors are usually evaluated because most of the methods available for frequency analysis compute both parameters.

The basic equation for frequency analysis is obtained from Equation (2.13) by neglecting damping and imposing the condition of free vibration

$$[K_s]\{X\} = \omega^2[M_s]\{X\} \tag{3.9}$$

where

$[M_s]$ - system mass matrix

$\{X\}$ - eigenvector corresponding to $\{w_s\}$ and ω^2

The symbols $[K_s]$ and ω have been defined earlier in the test.

Damping has only a negligible effect on the results (3), but it complicates the already involved solution even further by introducing complex frequency values. Therefore, it is common practice to

neglect damping when the frequencies and eigenvectors of structures are evaluated.

The solution to Equation (3.9) consists of evaluating the scalar values for ω^2 and the corresponding non-trivial eigenvectors $\{X\}$ for the given stiffness and mass matrix. The methods of frequency analysis can be divided into the transformation methods and iterative methods (8). The transformation methods are convenient for small sizes of $[K_s]$ and $[M_s]$ when all the frequencies and eigenvectors are desired. If the matrix size is large and only a few frequencies and eigenvectors are needed, as is in the case of finite element analysis, the iterative methods are advantageous.

In Equation (3.9) the stiffness and mass matrices are symmetric and often banded. Most methods require Equation (3.9) to be in the form of

$$[D_s]\{X\} - \omega^2\{X\} = \{0\} \tag{3.10}$$

where the dynamic stiffness matrix $[D_s]$ is defined by

$$[D_s] = [M_s]^{-1}[K_s] \tag{3.11}$$

Matrix $[D_s]$ is neither symmetrical nor banded and it may require more computer storage than the combined storage of the stiffness and mass matrices. Two methods have been found in the literature that do not require the formation of the dynamic stiffness matrix. The

first one, a transformation method based on Jacobi's diagonalization procedure, is described by Cooley and Lohnes (4, p. 31-59). It has been extensively used in this study and the computer listing is given in Appendix B. The second method, an iterative procedure developed by Fox and Kapoor (7), is particularly suitable for large matrix sizes when only a few of the smallest frequencies and corresponding eigenvectors are needed. The efficiency of the method depends on the quality of the initial estimates for eigenvectors. It has received only limited use in this study because of the difficulty with initial estimates for eigenvectors. Poor estimates usually require substantial amounts of computer time. However, the method can become very efficient once some experience with the prediction of eigenvectors is attained.

As pointed out in Section 3.1, only a part of the structure is often analyzed when the structure is symmetric. For frequency analysis, the nodal displacements along the symmetry axis must be carefully chosen to prevent a possible elimination of the significant modal shapes. Often more than one analysis needs to be performed to account for all the modal shapes. Several computations with a small matrix size usually are more economical than one computation with a large matrix size.

3.3. Dynamic Loading Function

Static live loads used for floor design given in current building

codes are simplified values representing not only static loads but also dynamic loads. These design loads are only useful for the static analysis, and a new load concept needs to be introduced for the dynamic analysis. The loads that cause undesirable vibrations in residential structures, such as impact loads due to walking and fallen objects, are of small magnitude. They do not structurally endanger the floor, but they excite vibrations that may be objectionable to humans. The walking of a single person, considered the most objectionable dynamic load acting on the floor (17), is chosen as the loading for the dynamic response analysis in this study.

Several empirical studies have been carried out to determine the forces applied to the floor by a foot during walking (9). The purpose of these studies has been either to measure the abrasion resistance of flooring materials to wear by foot traffic or to study the human locomotion to gather information for the design of artificial limbs. Harper et al., determined the force-time relationship for the vertical, horizontal and torque components of force caused by the foot pressure of a walking person (9). A typical graph from Harper's study, representing the vertical force-time relationship as shown in Figure 3.2, is used in this study as the forcing function for walking.

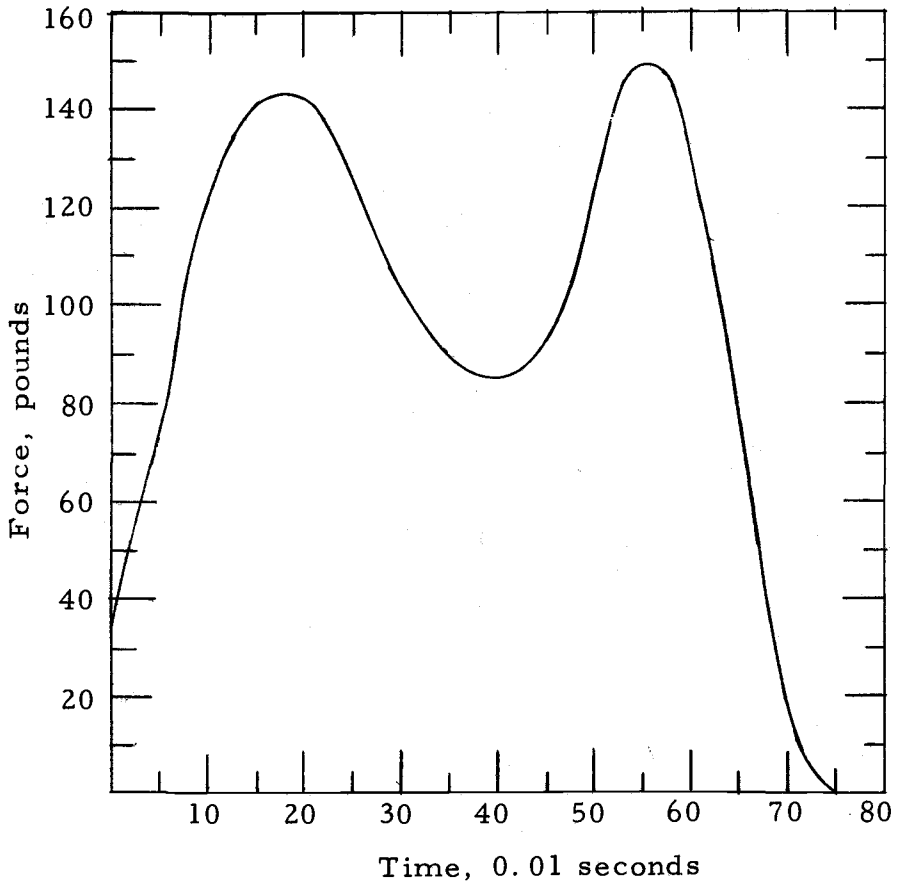

Figure 3.2. Forcing function for the human foot during walking.

3.4. Dynamic Response Analysis

The solution of the partial differential equations describing the structural motion is the primary concern of the dynamic response analysis. There are two general types of methods available; the rigorous approach and the numerical approach (3). The rigorous solutions are limited mostly to problems in which the loading and resistance functions can be expressed in simple mathematical forms. The numerical solutions are much more general and can be used to

evaluate not only linear elastic responses, but also non-linear responses due to any type of numerically definable loading function. The core of the numerical solution is the numerical integration of equations of motion for the successive time intervals. The displacement, velocity, and acceleration of the structure at the end of each interval are expressed in terms of their values at the beginning of the same interval. This procedure requires the definition of the acceleration or velocity change within the interval. The constant or linear acceleration methods are the most common choices, but more complicated procedures, such as Newmark's β method and various finite difference recurrence formulas may insure a greater stability of the procedure (3). A linear acceleration method is used in this study.

The choice of the time interval Δt greatly influences the stability of the numerical dynamic response analysis. To limit the round-off and truncation errors to tolerable amounts, Newmark recommends the range for Δt be about 1/6 to 1/5 of the shortest natural period (3). The highest modal frequency of a typical wood-joist floor for the types of finite elements used in this study can be as high as 1000 cps, resulting in a very small Δt; only a few ten thousandths of a second. Since the corresponding fundamental modal frequency is 20 to 30 cps, such a small interval demands several hundred intervals before significant data is obtained. The resulting

computation can require a considerable amount of computer time, especially for large matrix sizes.

The equations of motion can be expressed in terms of the acceleration, velocity and displacement as

$$[M_s]\{\ddot{w}_s\} + [C_s]\{\dot{w}_s\} + [K_s]\{w_s\} = \{P_s\} \tag{3.12}$$

where

$[C_s]$ - system damping matrix

Other symbols have been defined earlier in the text. Assuming a linear variation of the acceleration, the velocity vector at the end of the n-th interval is given by the following recurrence formula

$$\{\dot{w}_s\}_{(n)} = \{A\}_{(n)} + \frac{\Delta t}{2}\{\ddot{w}_s\}_{(n)} \tag{3.13}$$

where

$$\{A\}_{(n)} = \{A\}_{(n-1)} + \Delta t\{\ddot{w}_s\}_{(n-1)} \tag{3.14}$$

The subscripts in the parentheses denote the number of the interval.

The recurrence formula for the displacement vector is

$$\{w_s\}_{(n)} = \{B\}_{(n)} + \frac{\Delta t^2}{6}\{\ddot{w}_s\}_{(n)} \tag{3.15}$$

where

$$\{B\}_n = \{B\}_{(n-1)} + \Delta t\{A\}_{(n)} \tag{3.16}$$

The acceleration at the end of interval n is determined by the

substituion of Equations (3.13) and (3.15) into Equation (3.12)

$$\{\ddot{w}_s\}_n = [Q](\{P_s\}_{(n)} - [C_s]\{A\}_{(n)} - [K_s]\{B\}_{(n)}) \tag{3.17}$$

where

$$[Q] = [\,[M_s] + \frac{\Delta t}{2}[C_s] + \frac{\Delta t^2}{6}[K_s]\,]^{-1} \tag{3.18}$$

For linear systems, like the glued floors, Equation (3.18) remains constant for all the time intervals. The nailed floor behaves linearly only within certain deflection ranges (Figure 2.2), and the stiffness and damping matrix may require adjustments during the dynamic deflection. For each adjustment in the system matrices, a new matrix $[Q]$ must be evaluated, which requires a considerable amount of computer time for large matrices.

Initially, the displacement and velocity vectors are usually known. The acceleration vector at the beginning of the first interval is computed by the following formula

$$\{\ddot{w}\}_{(0)} = [M_s]^{-1}(\{P_s\}_{(0)} - [C_s]\{\dot{w}_s\}_{(0)} - [K_s]\{w_s\}_{(0)}) \tag{3.19}$$

For each additional interval, the acceleration vector is first determined by Equation (3.17) and vectors $\{A\}$ and $\{B\}$ follow using Equation (3.14) and (3.16), respectively. The velocity and displacement vectors need to be evaluated by Equation (3.13) and/or (3.15) only if required as an output.

Equations (3. 12) through (3. 19) were adapted from Reference 27 to conform to the notations used in this study and to be in a form most suitable for computer programming.

IV. TESTING OF THE METHOD AND THE COMPUTER PROGRAM

The element matrices developed in Chapter II, the methods of analysis presented in Chapter III, and the computer program given in Appendix B are verified in this chapter. Two types of verification, used at various stages during the development of this study, were performed. The first one consisted of analyzing previously solved problems by using the method developed in this study and comparing the results. The second type involved the finite element analysis of a laboratory tested floor and the comparison of the experimental and analytical results.

4.1. Comparison to Existing Solutions

Rectangular plates with various edge and loading conditions can be accurately analyzed using series solutions (22). Some of these solutions are used to verify the plate element matrices given in Appendix A and the analysis and computer program dealing with the assembly of plate element matrices and force vectors, the computation of static displacements and stresses and the two methods of frequency analysis used in this study.

A static displacement analysis was first performed for a square steel plate, shown in Figure 4.1a, to compare the centroidal deflection to the solution given by Reference 22. The plate, clamped along

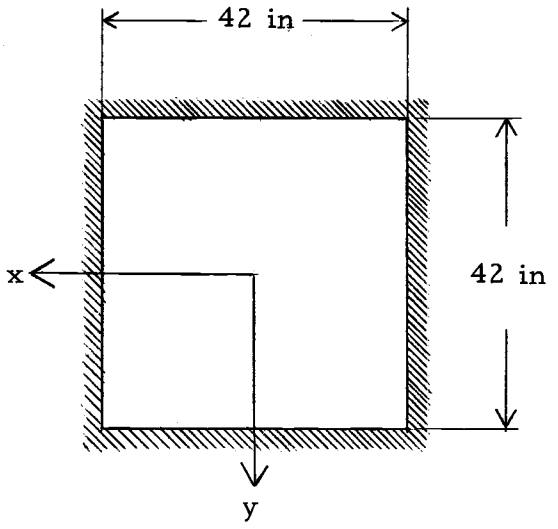

$h_p = 0.125$ in

$E_x = E_y = 3 \times 10^4$ ksi

$\nu_{xy} = \nu_{yx} = 0.3$

(a) Plate.

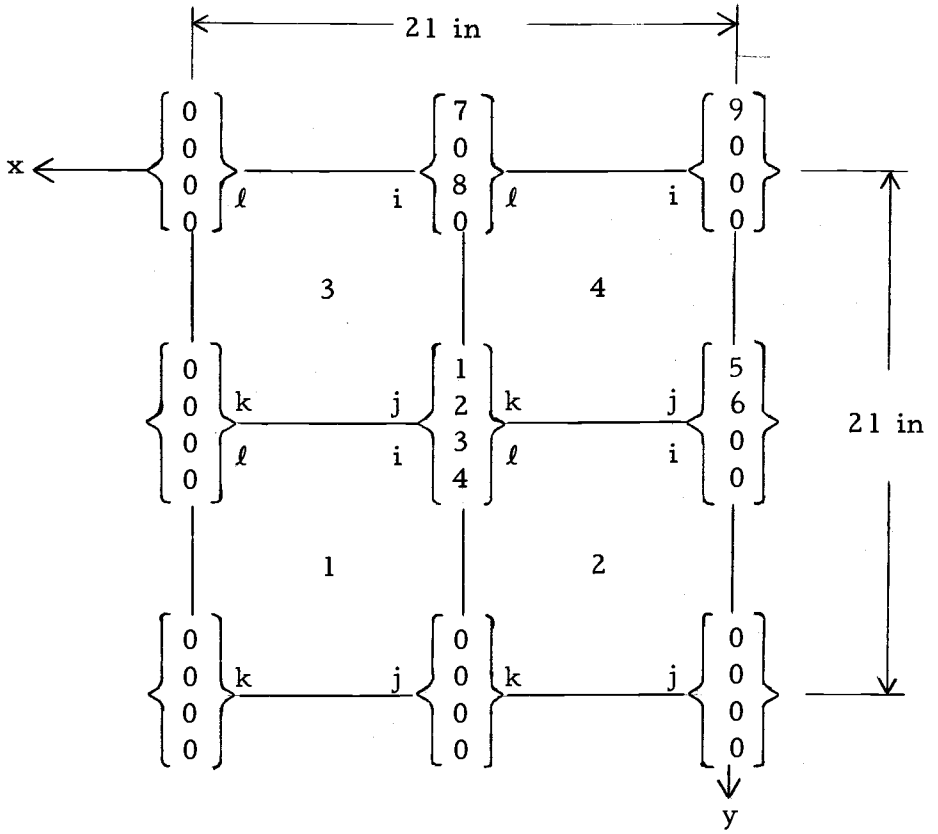

(b) Nodal displacement numbers for 4 element mesh.

Figure 4.1. Finite element model of a square plate.

all four edges, was loaded with a uniform load of 40 psf. Because of symmetry, only a quarter of a plate was analyzed, as indicated in Figure 4. 1b. Nodal displacement numbers of Figure 4. 1b are written in vector form corresponding to Equation (A. 15). A centroidal deflection of 0. 0255 in was obtained using the finite element method, which is within 0. 5% of 0. 0254 in; the result obtained in Reference 22. From this result, it was concluded that the plate stiffness matrix, defined by Equation (2.15), is correct.

McGlenn and Hartz extended the 12-degree of freedom bending plate element developed by Melosh to multilayered orthotropic plates (15). They analyzed a 7-layer plywood plate, clamped along the four edges and loaded with a vertical concentrated load at the plate centroid. The plate properties are the same as those shown in Figure 2. 1a except

E_x = 1, 500 ksi (determined by testing)

E_y = 94 ksi (determined by testing)

ν_{xy} = 0. 441 (from Reference 23)

ν_{yx} = 0. 023 (from Reference 23)

G = 117 ksi (from Reference 23)

Δh = 0. 1 in (layer thickness)

The same plate was analyzed using the 16-degree of freedom plate element given in Chapter II. In addition to the 4 element mesh shown

in Figure 4.1b, the centroidal displacement was also computed for the 16 element mesh. The results are shown in Figure 4.2. For the 4 element mesh the deflection computed according to this study closely agrees with that of McGlenn and Hartz. However, the agreement between the deflections computed by the two methods was not as good when the element mesh size was increased to 16. Both deflections approximately agree with the average test deflections, but the result by McGlenn and Hartz displays somewhat better agreement. The difference between the results obtained by the two methods is perhaps the result of the material properties used in the computation. Poisson's ratios and the shear modulus, taken from the handbook, influence the stiffness matrices derived in this study more than those used by McGlenn and Hartz. The surface stresses at the centroid of the plate, shown in Table 4.1, agree more closely, deviating not more than 7.4%.

Plate element stiffness matrices and the computer program for static displacement analysis were verified using the results of McGlenn and Hartz. The verification of the plate element mass matrix and the computer program for the frequency analysis was accomplished by analyzing rectangular orthotropic plates with clamped edges and comparing the results to known solutions. The frequency analysis of flexural vibration of rectangular orthotropic plates was first performed by Hearmon using the Rayleigh method (10) and subsequently

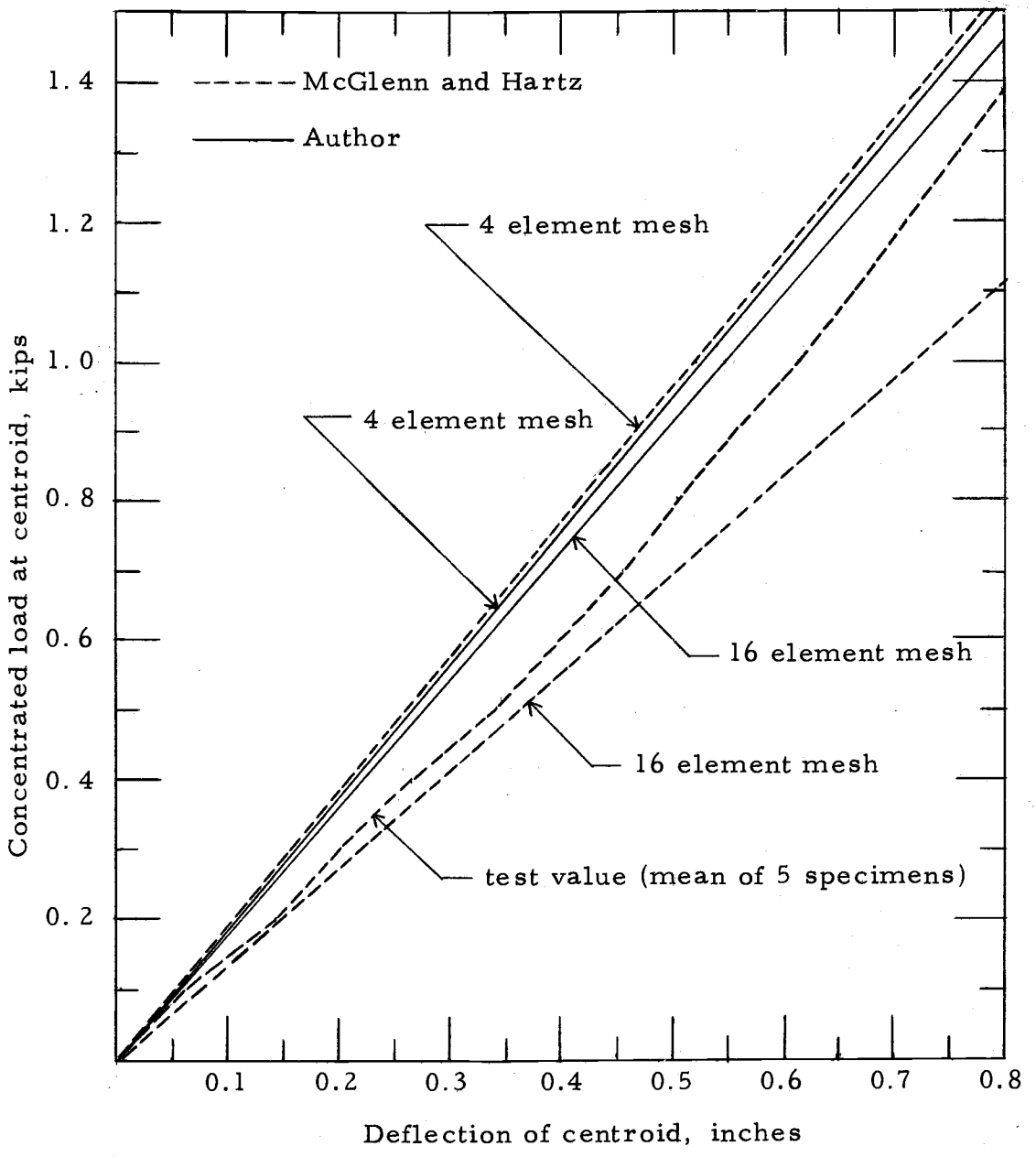

Figure 4.2. Deflection of a square orthotropic plate clamped along four edges.

by Dickinson using a sine series solution (6). Dickinson gives a frequency parameter γ for the lowest five modes of a square, clamped plate with the following properties

$$D_{11}/H = 1.543$$

$$D_{22}/H = 4.810$$

$$D_{12}/H = 0.186$$

$$D_{33}/H = 0.407$$

where

$$H = \nu_{xy} D_{22} + 2D_{33} \tag{4.1}$$

and

$$\gamma_m = \rho_p (2h_p)\omega_m^2 L^4/(\pi^4 H) \tag{4.2}$$

where

L - side length of square plate

Other symbols have been defined earlier in the text.

Table 4.1. Surface stresses of a square orthotropic plate.

Type	McGlenn and Hartz	Author
σ_x	3.30 ksi	3.055 ksi
σ_y	0.35 ksi	0.324 ksi

The same orthotropic plate was analyzed by the method developed in Chapter II and III. The lowest four frequency parameters γ obtained by the three methods are shown in Table 4.2. The kinds of

mesh used in the finite element analyses are shown in Figures 4.3 and 4.1b. Because the computer program according to Reference 4 failed to produce results for the mesh with 36 degrees of freedom shown in Figure 4.3c, the iterative procedure of Reference 8 was used. The first three modes were also computed on the basis of a quarter of the plate only, taking advantage of symmetry. For each mode, the choice of displacements along the symmetry axes was such as to force the plate into the desired modal shape. The results of Table 4.2 show very good correlation between the method used in this study and the series solutions by Dickinson, verifying the element plate matrices and the computer programs for the frequency analysis. The results of Table 4.2 also suggest that even a coarse element mesh usually gives a rather accurate value of the lowest modal frequency.

Table 4.2. Frequency parameter γ of a square clamped plate.

γ_1	γ_2	γ_3	γ_4	Source	Acc. to Mesh in Figure	Computer Program
35.71	96.42	207.03	280.69	Dickinson		
36	98	219	--	Hearmon		
37.14	146.8	--	--	Author	4.3a	NATFREQ
36.02	99.71	215.4	305.4	Author	4.3b	NATFREQ
35.90	---	--	--	Author	4.3c	EIGENV
35.77	97.03	210.20	--	Author	4.1b	NATFREQ
---	98.72	207.40	--	Author	4.3d	NATFREQ

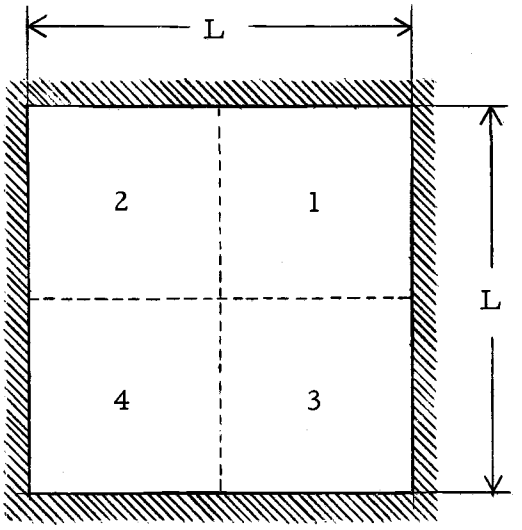

(a) Complete plate, 4 mesh

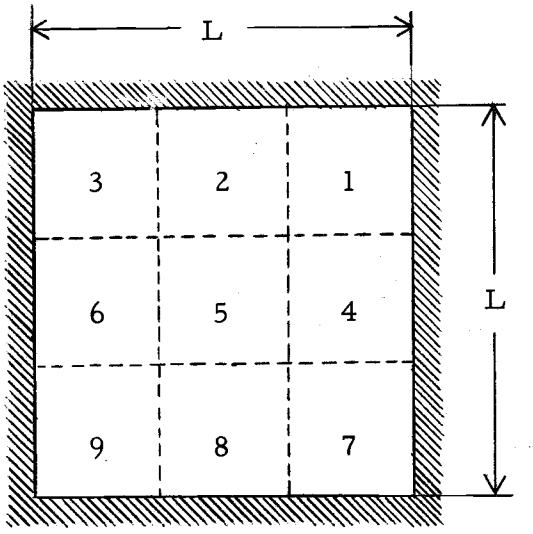

(b) Complete plate, 9 mesh

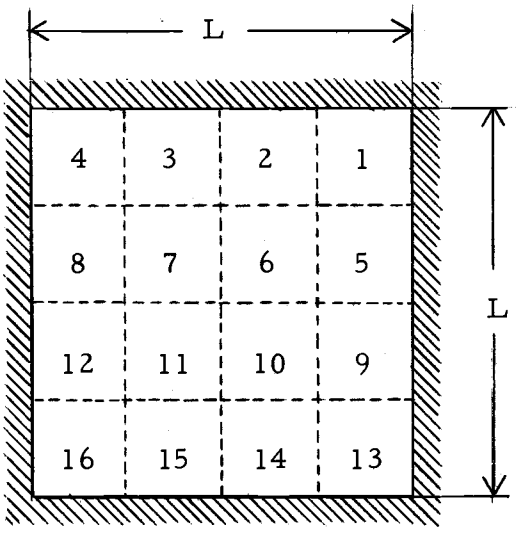

(c) Complete plate, 16 mesh

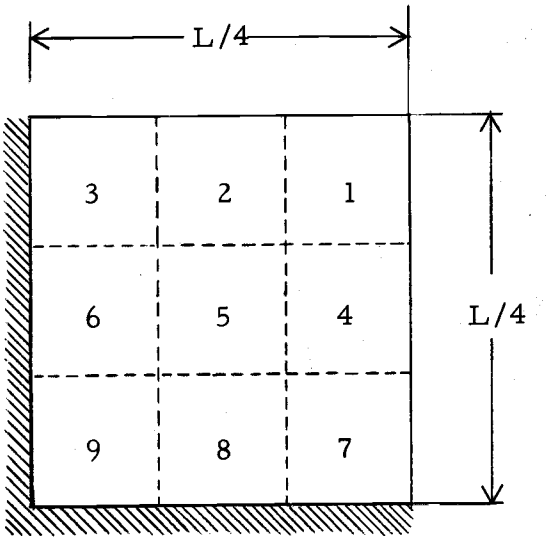

(d) A quarter of the plate, 9 mesh

Figure 4.3. The kinds of finite element mesh used for frequency analysis.

Long and narrow rectangles are a very convenient shape for the plate finite elements for joist floors. To investigate if long and narrow finite elements affect the results, a frequency analysis was performed on a simply supported orthotropic plate shown in Figure 4.4. The plate is one-half inch Douglas fir plywood with 5 plies of 0.1 in thickness. The grain direction of the surface layers is parallel to the y axis. Only the 4 element mesh is shown in Figure 4.4, but the 6 and 8 element mesh also were analyzed. The element width b was 16 in for all the three mesh choices. The frequencies, shown in Table 4.3, agree with those of Hearmon. The normal behavior of the results indicate that the use of long and narrow elements will present no difficulty.

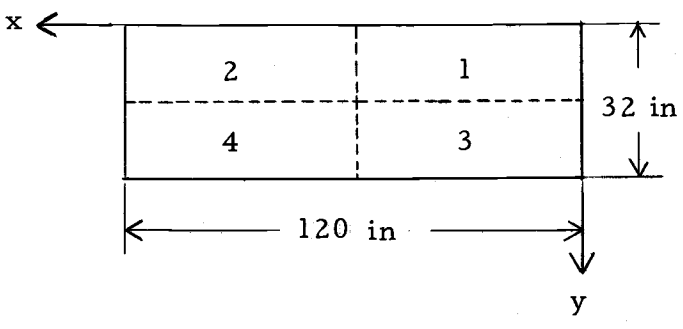

E_x = 2,150 ksi
E_y = 108 ksi
G = 168 ksi
ν_{xy} = 0.499 ksi
ν_{yx} = 0.029 ksi

Figure 4.4. Rectangular plywood plate simply supported along all four edges.

Table 4.3. The lowest three modal frequencies, in cps, of a rectangular plate.

ω_1	ω_2	ω_3	Mesh	Source
42	45	49		Hearmon
43	47	101	4	
43	46	53	6	Author
42	44	47	8	

4.2. Comparison to an Experimental Floor

Recently an extensive experimental investigation was conducted in the Forest Research Laboratory, Oregon State University, to evaluate the response of wood-joist floors to static and dynamic loads. A floor from this experimental investigation was analyzed by the finite element method. The comparison of the analytical and experimental results was then used to verify the composite beam element matrices, the overall finite element model of the floor, the method of analysis used, and the corresponding computer program.

The arrangement of the experimental floor is shown in Figure 4.5. Douglas fir joists of nominal size, 2 in by 6 in, were visually graded as Standard and better according to the rules of the West Coast Lumber Inspection Bureau applicable at that time[1/](24). The joist moduli of elasticity, shown in Table 4.4, were obtained by loading each joist in bending according to ASTM Standard Method D198-67 (2). Other joist properties listed in Table 4.4 are the width and height, based on the midspan cross-section, and the weight per linear foot, determined by weighing.

[1/] The former Standard grade approximately corresponds to the new No. 2 grade.

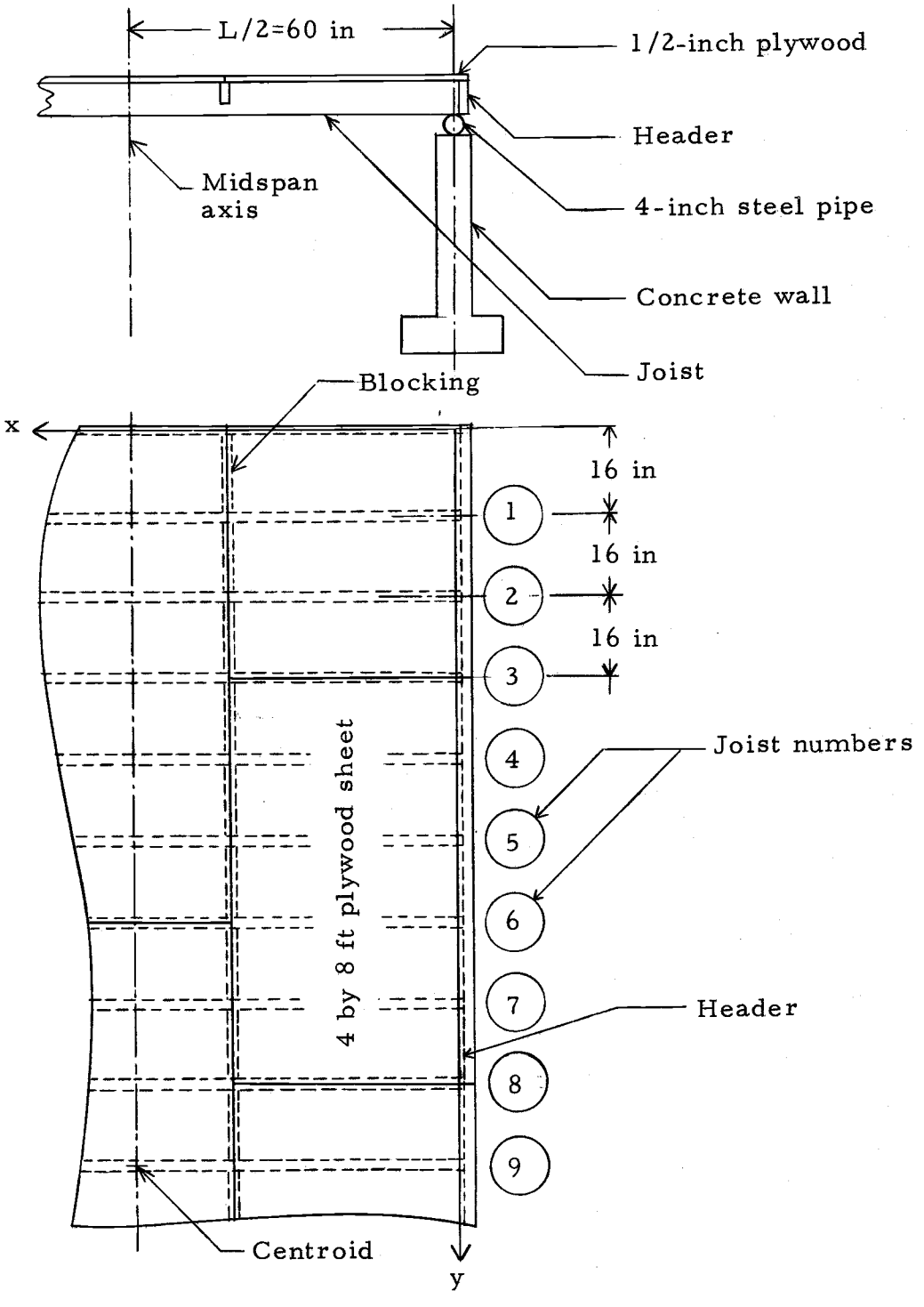

Figure 4.5. Arrangement of experimental wood-joist floor.

Table 4.4. Properties of joists and nail connection.

Joist Properties					Nail Joint Properties	
Joist No.	Width in	Height in	E ksi	Weight lbs/ft	k psi	f_k
1	1.570	5.258	1,973	1.87	543	1.41
2	1.559	5.159	3,141	2.07	558	1.58
3	1.540	5.367	2,052	1.97	552	1.72
4	1.577	5.173	2,132	1.70	527	1.73
5	1.563	5.186	2,250	1.71	527	1.71
6	1.575	5.347	1,825	1.83	541	1.79
7	1.557	5.286	2,031	1.86	541	1.74
8	1.577	5.294	1,947	1.92	547	1.74
9	1.556	5.353	1,985	1.76	535	1.73
10	1.592	5.352	1,520	1.80	538	1.86
11	1.594	5.339	1,573	1.77	535	1.86
12	1.541	5.217	2,581	1.95	550	1.66
13	1.588	5.333	1,999	1.86	541	1.74
14	1.575	5.251	2,077	1.75	532	1.73
15	1.574	5.245	2,236	1.87	543	1.70
16	1.578	5.275	2,251	1.88	543	1.71
17	1.575	5.297	2,035	1.75	532	1.40

The floor was covered by 1/2-inch, 5-ply, C-D structural interior grade Douglas fir plyscord plywood. The ply thickness of 0.0987 in, based on the average randomly measured plywood thickness, was assumed to be the same for all the plies. The modulus of elasticity along the grain of veneer, E_L, was determined from 15 bending tests conducted on 1 in wide and 18 in long beams cut from plywood sheets. In evaluation of E_L, the following handbook ratio (23) was used

$$E_T = 0.06E_L \tag{4.3}$$

where

E_T - modulus of elasticity in the tangential direction of wood

The handbook values (23) were used to determine the remaining elastic properties. The weight per square feet of plywood, w_g, was obtained by weighing 10 randomly selected sheets. The plywood properties used in the theoretical analysis are

$$E_L = 1,917 \quad \text{ksi}$$

$$E_T = 117 \quad \text{ksi}$$

$$G = 150 \quad \text{ksi}$$

$$\nu_{LT} = 0.441$$

$$\nu_{TL} = 0.023$$

$$w_g = 1.253 \quad \text{psf}$$

It should be noted that the corresponding handbook value (23) of E_L at a moisture content of 7.5% and a specific gravity of 0.506 is 1,950 ksi, which is within 2% of the E_L obtained by testing.

The general construction of a test floor is shown in Figure 4.5. The joists, spaced at 16 in, were butt-nailed to the headers with 16d common nails. Nominal 2 in by 4 in blocking, toenailed to each joist to support plywood edges, provided the continuity along the x axis in the plywood plate. The plywood was laid with staggered joints with its longer side and the surface grain direction parallel to the y axis.

The plywood was then nailed to the joists and blocking using 8d common nails; edge nail spacings were 6 in and intermediate spacings were 10 in. The whole structure was supported by two, 4 ft high concrete walls.

In additon to physical and geometric properties of the floor components, the effective width of the T-beam and the stiffness reduction factors due to nail slip must be determined. The effective width for the complete composite action, as determined by Reference 1, is primarily influenced by the joist spacing to span ratio and by the elastic properties of the plate and joists. If the plate is stiffer in the y direction than in the x direction and if the spacing to span ratio is less than 0.1, as it is in the floor analyzed, the effective width is about equal to the spacing. Therefore, the effective width is taken as 16 in.

The stiffness reduction factor f_k, determined from the diagrams in Reference 13, depends not only on the properties of the joists and the plate, but also on the modulus of the shear connector k determined by Reference 25. The evaluation of the factors f_k and k is somewhat cumbersome, since they must be evaluated for each joist, but it presents no problem. The value of f_k and k for individual joists are given in Table 4.4.

The assumption used in the analysis that the plywood plate is fully continuous in the x and the y directions violates the true

conditions, since no bending moments are transferred through the edges of individual plywood sheets (Figure 4.5). However, the errors associated with this violation are considered to be negligible. The plate resistance bending moment in the x direction is extremely small in comparison to the beam resisting moment and can easily be neglected. The major stiffness contribution of the plate in the x direction is associated only with the membrane forces which are fully transferred through the blocking. In the y direction, partial discontinuities in the resisting bending moments at every third joist (Figure 4.5) are accompanied by the full transfer of the vertical shear through the nails along the plywood edges. This shear transfer reduces the errors due to discontinuity in the y direction to tolerable limits. The results of the static displacement analysis for the experimental floor demonstrate that the assumption of the full continuity in the plywood floor covering is justified.

The blocking is considered only as being a support to the plywood edges and its contribution to the stiffness is neglected. Similarly, the effect of headers is not included in the finite element analysis.

The results of two static tests and one dynamic test, performed on the experimental floor, were used to verify the method of this investigation. A brief description of the tests follows; a detailed description can be found in Reference 18. The first static test, called

a concentrated load test, was conducted by placing a concentrated load of 300 lbs at midspan of a joist and then recording the midspan deflections of all the joists. In the second static test, identified as an ultimate load test, a uniform load was applied to the floor at a step-wise rate of 10 psf per 10 minutes until the floor failed. For each load increase of 10 psf, midspan deflections of all the joists were recorded. The dynamic test was a flexural, free vibration test. The free vibration was induced by the initial deflection caused by a 200-pound load placed at the floor centroid. The midspan vibration of each joist was monitored to give the time-deflection traces.

The analysis of the floor was performed under the same loading conditions as those imposed in testing. The deflections and stresses due to the concentrated load and the uniform load, computed by the static displacement analysis, were compared to the results of the static tests. The midspan deflections at successive time intervals, computed by the dynamic response analysis, were compared to the time-deflection traces of vertical free vibration tests.

The finite element mesh and the displacement numbers used in the static analysis are shown in Figure 4.6. The experimental and computed midspan deflections caused by a 300-pound load placed at the midspan of joist 7, shown in Figure 4.7, agree closely. It should be noted that the experimental deflections were recorded to 0.01 in accuracy with the last digit being estimated. The stresses in the

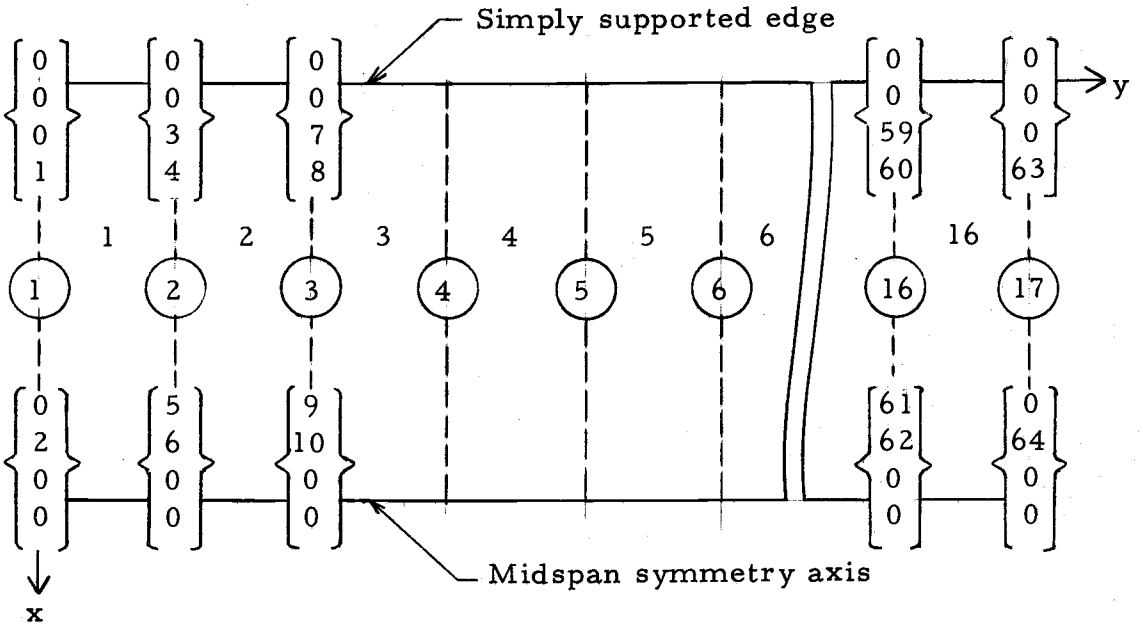

Figure 4.6. Finite element mesh for floor analysis.

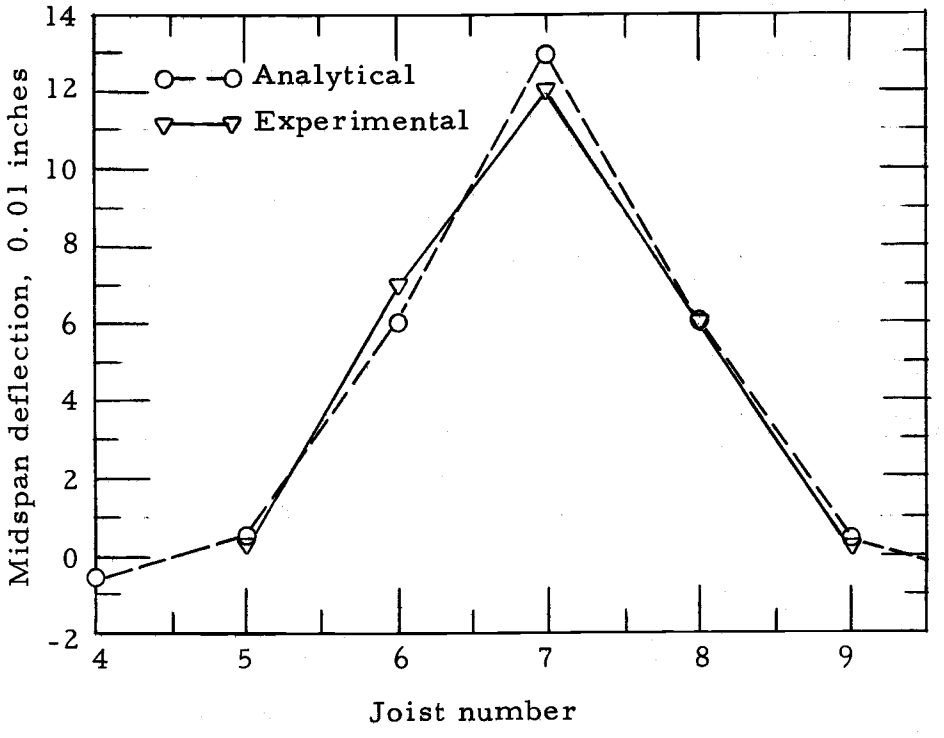

Figure 4.7. Comparison of analytical and experimental deflections due to a 300-pound concentrated load applied at joist 7.

extreme fibers for the same loading are given in Table 4.5. Because no strains were measured during testing, only analytical stresses are given.

Table 4.5. Midspan stresses due to a concentrated load applied at joist 7.

Joist No.	4	5	6	7	8	9	10
σ_x, psi	-34	35	347	900	365	26	-28
σ_y, psi	68	-228	-1,240	-1,558	-1,570	-1,224	224

The results of the static displacement analysis of the test floor for the uniform load of 50 psf were compared to the corresponding experimental values in Table 4.6. Since the test floor had two more joists than the analyzed floor, midspan deflections of only 11 intermediate joists are shown. The mean computed deflection deviates less than 2% from the mean experimental deflection. The maximum individual deviation of about 12% is for joists 10 and 11. As shown in Table 4.4, the moduli of elasticity for these two joists are considerably below the average, which is reflected by the large analytical deflections of the two joists (Table 4.6). Smaller rigidities of joists 10 and 11 are not reflected in the experimental deflections, possibly because of the higher local stiffness in the plywood. Wood is a highly variable material, and the maximum differences between the experimental and analytical values of about 10% are thought normal,

Table 4.6. Midspan deflections and stresses due to a uniform load of 50 psf.

Joist Number	4	5	6	7	8	9	10	11	12	13	14	Mean
Experimental deflection, in	0.33	0.34	0.33	0.34	0.35	0.34	0.34	0.33	0.32	0.33	0.31	0.33
Analytical deflection, in	0.336	0.333	0.338	0.334	0.332	0.347	0.381	0.368	0.317	0.314	0.330	0.339
Stress in joists σ_x, psi	1,086	1,144	953	1,052	1,009	1,092	888	879	1,267	978	1,057	---
Stress in plate σ_y, psi	-212	-54	-83	-66	-40	-195	-406	-171	-593	-51	-205	---

especially when the average differences are much smaller.

The computed stresses are also shown in Table 4.6. The stress σ_y reflects the variation in joist stiffnesses; large differences in stiffness in adjacent joists produces large values of σ_y.

The correlation between the experimental and analytical values of Figure 4.7 and Table 4.6 is satisfactory. Therefore, the finite element model for the static analysis of wood-joist floors and the corresponding computer program are verified.

Since the damping matrix used in this study is assumed to depend on the lowest modal frequency, and since the time interval, used in the dynamic response analysis, is a function of the highest modal frequency, the frequency analysis for the experimental floor has been performed before the response analysis. The computer program, used for the frequency analysis, can compute the frequencies only for matrix sizes less than 35, which is too small to analyze the whole experimental floor at once. Therefore, the frequency analysis was performed for the three different sections of the floor; the first floor section was the original floor from joists 2 through 10 (Figure 4.5), the second and the third section consisted of joists 5 through 13 and joists 8 through 16, respectively. The assumption was that these three analyses detected the lowest and highest modal frequencies of the floor consisting of joists 2 through 16 for which the response analysis was performed. The finite element mesh used in the

frequency analysis was like the one in Figure 4.6. The results, listed in Table 4.7, show that the highest modal frequencies are the same for all of the three sections analyzed and that the corresponding lowest frequencies do not differ much. The value of 25.3 cps was used in the formulation of the damping matrix and the value of 783 cps was inverted and divided by 6 to give the time interval of 0.00025 second for the dynamic response analysis.

Table 4.7. Ranges of modal frequencies.

Floor Section Analyzed	Joist 2 to 8	Joist 5 to 13	Joist 8 to 16
ω_{30}, cps	783	783	783
ω_1, cps	26.2	25.3	25.4

The damping ratios, selected according to Reference 26, were 0.7 and 1.5% of critical damping for the plate and the composite T-beams, respectively. The value of 0.7% is twice the material damping in order to compensate for damping along the plywood edges and in the plywood-blocking connections.

The finite element mesh for the dynamic response analysis was that as shown in Figure 4.6, except that some of the end joists were removed. The static displacements due to the 200-pound load applied at the floor centroid, computed by the matrix displacement analysis, were the initial displacements starting the vibration. The dynamic

response analysis was performed for two floors; the first one having joists 2 through 16 and the second one having joists 7 through 11. The results are shown in Figure 4.8 in the form of time-displacement traces of a joist midspan at the centroid. The comparison between the analytical and experimental values is very poor because of the changes in damping and stiffness during the vibration. To investigate the effect of damping, the five-joist floor also was analyzed with 1.5% and 3% of critical damping for the plate and composite beam, respectively. This change in damping reduced the amplitude but did not improve the correlation.

The poor correlation between the experimental and analytical results can be explained by a cyclic load diagram like the one in Figure 2.2, but with the positive-negative load cycling. Such a diagram, showing the load-slip looping after the hundredth cycle, has been deduced from Figure 2.2 and is given in Figure 4.9. As in Chapter II, the analogy is made between this diagram and the conditions in the nailed plywood-joist connection. Initial static deflection causing the vibration corresponds to point 1 in Figure 4.9. During the upward motion of the floor, bearing in the nails decreases accompanied with increased slip until the contact between the nails and wood is broken (point 2). This probably happens before the floor reaches its neutral position, i.e., the position of zero deflection. While the floor moves through the neutral position, pure slip is taking place and

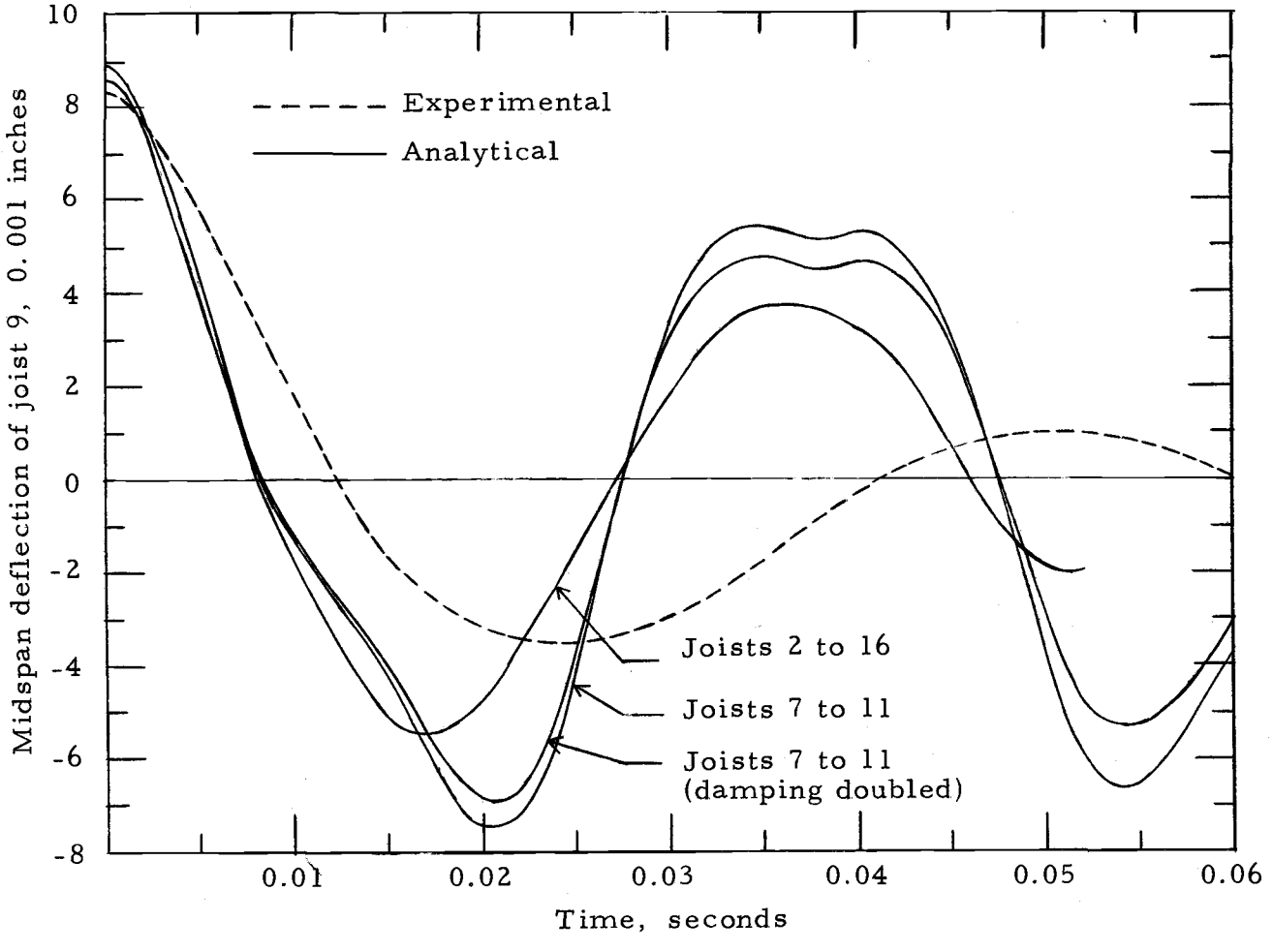

Figure 4.8. Dynamic response of a floor to initial displacements.

no shear is transferred. In this stage no composite action exists between the plate and joists and the stiffness matrix is reduced to that of bending only. At the same time the damping ratio of the beam can become more than 10%, the value given by Reference 26 for zero nail bearing. Sometime during the upward deflection the connection is made between the wood and nails (point 3), and the nails start to transfer more and more shear, resulting in an increase of stiffness and a decrease of damping. After the floor reaches its uppermost position (point 4) a similar mechanism takes place during the downward deflection. In the dynamic response analysis, the stiffness and damping matrix were constant. In Figure 4.8, a decrease in stiffness during vibration is indicated by the phase shift of the experimental trace in relation to the analytical traces. The tenfold increase in damping ratio is indicated by the smaller amplitudes of the experimental trace.

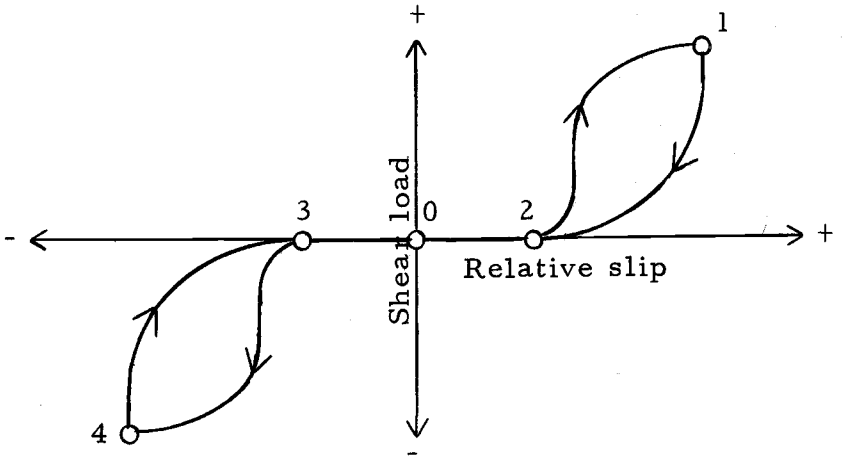

Figure 4.9. Cyclic load-slip curve of nailed plywood-joist connection.

The dynamic response analysis used in this investigation should give good results for floors with rigid plywood-joist connections, but modifications are necessary when these connections are semi-rigid. However, no experimental study could be found on the exact nature of the slip mechanism shown in Figure 4.9.

4.3. Convergence

The finite element formulation based on Hermitian polynomials results in solutions that monotonically converge from the stiffer side toward their true values (16). The results shown in Figure 4.2 and Tables 4.2 and 4.3 demonstrate the convergence for the solutions of the static displacement and the frequency analyses of orthotropic plates. To investigate the convergence for floors, a separate static displacement analysis was performed for a simply supported floor with 4 joists. The floor properties are the same as those of the experimental floor of Section 4.2 between joists 9 and 12 with the following changes: the value of E for joist 9 is replaced by 1,556 ksi and the new values for the stiffness reduction factors are 1.38, 1.35, 1.35 and 1.30 for joists 9, 10, 11 and 12, respectively. The kinds of finite element mesh used are shown in Figure 4.10. The floor was loaded by a uniform load of 40 psf and a concentrated load of 600 lbs applied at the midspan of joist 9. The results are shown in Table 4.8.

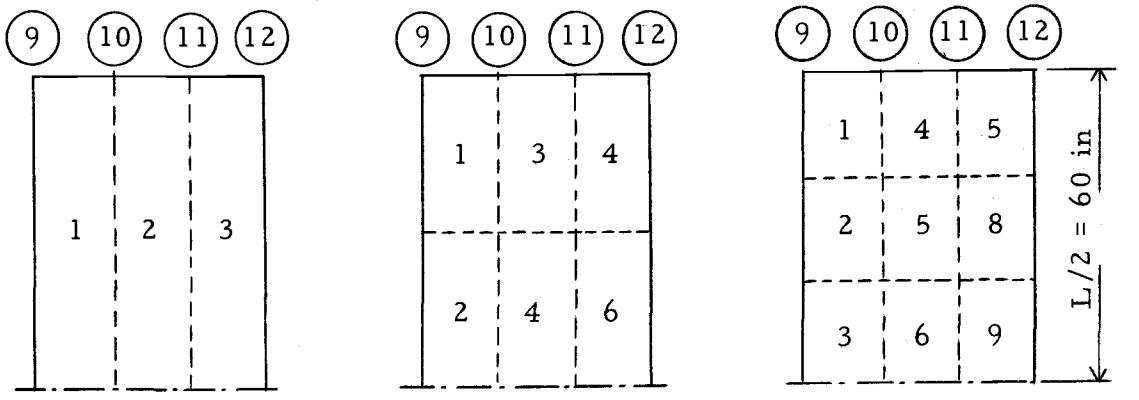

(a) 3 mesh (b) 6 mesh (c) 9 mesh

Figure 4.10. Finite element mesh of a floor with four joists.

Table 4.8. Midspan deflections and stresses.

Joist Number		9	10	11	12
Deflection, in	3 mesh	0.6874	0.3557	0.2085	0.0937
	6 mesh	0.6875	0.3551	0.2087	0.0938
	9 mesh	0.6882	0.3564	0.2093	0.0937
Stress in joists, σ_x, psi	3 mesh	1,842	1,143	680	434
	6 mesh	1,821	1,024	605	388
	9 mesh	1,820	1,004	594	379
Stress in plywood, σ_y, psi	3 mesh	-212	-3,736	-1,660	-273
	6 mesh	-232	-3,742	-1,650	-276
	9 mesh	-235	-3,734	-1,670	-277

Deflections and stresses in Table 4.8 indicate a convergence toward a more flexible solution as indicated by increasing deflection. That the deflections at joist 12 slightly decrease because of the mesh

refinement does not indicate a stiffening of the floor, since a concentrated load at joist 9 moves joist 12 upward.

Because deflections and maximum stresses changed only slightly when the number of finite elements was tripled, the finite element mesh shown in Figure 4.10a is probably satisfactory for most conditions encountered in the design of wood-joist floors.

V. DISCUSSION AND CONCLUSIONS

The finite element method and the computer program, developed in this investigation, can be used to compute static and dynamic deflections and stresses not only for simply supported joist floors, but also for continuous floors and overhanging floors. For some floor types the computer program can be used as shown in Appendix B; for others, minor modifications may be necessary. Additional experimental information on the properties of some floor types is still needed in order to apply the method as a design tool. The advantages and limitations of the method, application for the method, and recommendations for future studies are discussed in this chapter.

5.1. Discussion of the Method

The objective of this investigation, to develop a theoretical procedure and a computer program for static and dynamic analysis of wood-joist floors, has been achieved. The procedure is based on available theoretical and empirical developments. The use of the finite element method has afforded a solution to the general problem for which in the past only a few simple cases have been solved. Therefore, the simplifications in the currently used simple beam method of joist floor design are no longer necessary. Floor elements can be of any material or combination of materials with known elastic,

mass and damping properties. The joist rigidities and masses can vary, the floor covering can be isotropic or orthotropic, and the connection between joists and floor coverings can be rigid or semi-rigid. Types of floor supports or boundary conditions present no difficulty except for possible minor modifications in the computer program. Not only static concentrated loads or static distributed loading according to an arbitrary function may act on the floor, but also dynamic loads which vary with time according to numerically or mathematically defined functions.

For the static displacement analysis, the finite element model consisting of plates and T-beams resulted in displacements which had an average deviation of less than 2% from the experimental displacements, which is usually tolerated for materials as variable as wood. This deviation was observed for relatively coarse finite element mesh, i.e., finite elements were long strips consisting of half-span long T-beams and plates with the plate element width being equal to the joist spacing. The approximate solution to the problem of coupling between the bending and membrane and/or axial forces applied in this investigation needs no further refinement; the rigorous treatment of the coupling would unnecessarily increase the accuracy beyond the limits which are significant for the design of ordinary residential floors.

The use of the plate and T-beam finite element model in the

dynamic response analysis resulted in a poor correlation between experimental and analytical results. The experimental floor had nailed connections between the joists and the floor covering, which introduced not only elasto-plastic behavior of T-beam elements, but also large variations of damping during the floor vibration. Because the model analyzed was assumed to be linearly elastic with constant damping throughout the floor vibration, the analytical and experimental results could not match. The shift in phase and the decrease in amplitudes on the experimental time-deflection trace (Figure 4.8) reflect these changes in stiffness and damping. Modification of the dynamic response analysis and the computer program can be made to account for the changing stiffness and damping once the appropriate experimental data are available.

Since the assumption of constant stiffness and damping is not violated for glued floors with rigid connections between the joists and the floor covering, the results of the dynamic response analysis should be much better for glued floors than for nailed floors. No comparison between experimental and analytical results was made for glued floors, because no experimental data were available.

The finite element matrices for the bending plate elements developed in Appendix A can also be used to perform the static and dynamic analysis of rectangular isotropic and orthotropic plates. As in the case of joist floors, no restrictions are imposed on the plate

analysis as to the boundary conditions, material properties and loading. The plate problems solved were in very close agreement with the existing solutions used in the comparison; agreements of about 0.1% were achieved in natural frequencies in the third refinement of the finite element mesh (Tables 4.2 and 4.3).

The energy expressions in Section 2.2 and the development of the plate element matrices in Appendix A are general and they can be used to develop the element matrices for other displacement functions used to describe the plate bending displacements. An immediate application would be the development of the plate element matrices for the sixth order Hermitian polynomials adding w_{xx} and w_{yy} to the displacement vector. The resulting matrices of size 36 can be reduced to size 16 or 12 using the matrix condensation suggested by Pestel (16). Similar matrix condensations performed by Pestel on beam element matrices resulted in matrices that gave faster convergence than the non-condensed matrices of the same size formed by lower order polynomials (16). It is likely that the matrix condensation would also accelerate the convergence for the plate matrices.

Some of the problems used for the method verification in Chapter IV were tested for convergence. The successive element mesh refinements brought about a rapid convergence of not only the plate modal frequencies (Tables 4.2 and 4.3) but also the floor static deflections and stresses (Table 4.8). The roughest mesh used often

gave the desired accuracy.

5.2. Discussion of Applications of the Method

The method developed in this investigation can be used either as a substitute for proof testing or as a tool to modify the existing design method for wood-joist floors. The proof testing of full size structures, performed to find out if a certain structural type conforms to existing building codes, is an expensive procedure giving specific results pertaining only to the type tested. Savings in time and money can be achieved by applying an analytical procedure instead of the proof testing and using the testing only to establish the properties of the floor components. The suggested modification of the existing design method consists of modifying the allowable joist properties, i.e., moduli of elasticity and stresses, while retaining the existing simplified method of the floor design. Since the nature of this modification is more complicated than the problem of proof testing, the factors associated with the modification are discussed in more detail.

The allowable properties for a grade and species of joists are based on the clear wood properties modified for factors such as growth defects, moisture content, duration of load and safety factor (2). The factors accounting for the T-beam composite action and the support that the stiffer joists in the floor give to their more flexible neighbors can be established using the analytical procedure developed

in this study and then applied to the existing allowable properties.

Each grade and species of joists is associated with a statistical probability distribution for each of its properties. Assuming that this distribution follows a Gaussian probability function, it can be defined by the average and the standard deviation, i.e., by the two parameters which can easily be found in the literature. The probability distributions of the joist stiffnesses can be used to modify the existing floor design if the deflection limitations prevail, as for the floor with joists of grades No. 1 and No. 2 (24). The procedure suggested for this modification is next outlined for a floor with a certain joist type. Joist stiffnesses are randomly selected from the stiffness probability distribution of a joist type considered and assigned to predetermined joist positions in a previously identified group of floors. The population of floors formed in this way represents all the floors of a type being modified. For each of these floors, the maximum deflection at the working load is computed by the finite element method developed in this investigation and by the simplified single beam method. The modulus of elasticity, E_s, that gives the same deflection by the simplified method as the maximum deflection computed by the finite element method is given by

$$E_s = E_a w_s / w_f \qquad (5.1)$$

where

w_f - maximum deflection at working load computed by the finite element method

w_s - maximum deflection at working load computed by the simplified method

E_a - allowable modulus of elasticity

All the values of E_s form the probability distribution. Since E_a is an average value for a species and grade of joists (2), the average value for the E_s-distribution should be the new allowable modulus of elasticity, to be used in conjunction with the simplified method of floor design. The value of E_s not only depends on the species and grade of joists, but also on the properties of floor covering and shear connector modulus. Therefore, a large number of floor types must be evaluated in this manner even if only a few of the most important types of floors are considered.

The design of floors using lower grades of lumber, such as No. 3, is often governed by the allowable stresses. A new allowable stress for a grade and species of joists can be determined by a procedure similar to that of E_s. In this case the necessary probability distribution is a population of load-deflection relationships, which can be determined experimentally and/or from past studies. From this distribution, a population of floors is formed as in the case of the

stiffness modification, except that the joists are now represented by their load-deflection relationships. A finite element displacement analysis is performed for each floor. A uniform load, applied to the floor, is increased in steps until one of the joists fails, at which load level the maximum stress of the failed joist, σ_m, is computed. All the values of σ_m form the probability distribution. Applying the procedure recommended by the American Society for Testing and Materials (2), the allowable modified stress for a grade and species is equal to the value of σ_m at the 5% point of the weaker side of the probability distribution divided by the safety factor. This modified allowable stress accounts also for the T-beam action and the effect of the floor indeterminacy, and it is larger than the corresponding existing working stress, which is based on the properties of joists only. At higher load levels, the load-deflection relationship of joists becomes non-linear, which can adequately be represented for most joists by a bi-linear relationship. The computer program given in Appendix B was developed for the linear load deflection relationship, but can easily be modified to account for a defined non-linear relationship.

5.3. Conclusions and Recommendations

Two types of conclusions have been reached on the basis of this investigation; the first type pertains to the method of analysis

developed in this investigation and the second type deals with the structural behavior of wood-joist floors. The most important conclusions are

1) The joist floor can be represented by a finite element model consisting of bending plate elements and composite T-beam elements.
2) Static displacement analysis of an experimental floor resulted in a good correlation between the analytical and experimental deflections.
3) Dynamic response analysis and the corresponding computer program can be used to analyze rigid glued floors, but must be modified for nailed floors.
4) Static displacements and modal frequencies of orthotropic plates computed by the finite element method agree closely with the results of other investigators.
5) The fourth order Hermitian polynomials used for finite element displacement functions result in sufficient accuracy.
6) For a simply supported floor, a mesh with a single finite element along the half-span results in sufficient accuracy.
7) The procedure for the development of the finite element matrices for the plate bending element applied in this investigation can be used for other displacement functions.
8) The finite element procedure developed can be used not only

to analyze wood-joist floors but also joist floors made of concrete, steel and combinations of concrete, steel and wood.

9) Nailed floors deform elastically if loaded statically, but follow an elasto-plastic deformation pattern if loaded dynamically.

10) Rigidly glued floors deform elastically if loaded statically or dynamically.

11) Properties of nailed joist-plywood connections necessary for the static displacement analysis can be determined on the basis of existing studies.

12) Rotational discontinuities in the plywood floor covering can be neglected.

This dissertation has uncovered the need for several studies. The essential recommended studies are

1) An experimental study to establish the relationship between the slip and cycling load (Figure 4.8), as well as the variation of stiffness and damping during the cycling.

2) An experimental study on the probability distribution of the complete load deflection relationship for the most important grades and species of joists.

3) An experimental study to determine floor damping due to interlayer friction caused by vibration waves across the span, friction between the edges of the adjacent plywood sheets, and

the support friction.

4) Applying the method developed in this study and the statistical procedure outlined in Section 5.2, computation of new allowable values for stresses and moduli of elasticity for the most important floor types.

5) An experimental study to determine acceptable levels of floor vibration with respect to human response to vibration.

6) A modification of the method and the computer program developed in this study to account for elasto-plastic behavior of floors.

7) A modification of the computer program developed in this study to accommodate larger matrices.

BIBLIOGRAPHY

1. Amana, E.J. and L.G. Booth. Theoretical and experimental studies of nailed and glued stressed-skin components: Part I. Theoretical study. London, Journal of the Institute of Wood Science 4(1):43-69.

2. American Society for Testing and Materials. 1970 book of ASTM standards. Part 16. Philadelphia, 1970. 894 p.

3. Biggs, John M. Introduction to structural dynamics. New York, McGraw-Hill, 1964. 341 p.

4. Cooley, William W. and P.R. Lohnes. Multivariate procedures for the behavioral sciences. New York, Wiley, 1962. 211 p.

5. Clough, Ray W. and J.L. Tocher. Finite element stiffness matrices for analysis of plate bending. In: Proceedings of the First Conference on Matrix Methods in Structural Mechanics, Report no. AFFDL-TR-66-80, Wright-Patterson Air Force Base, 1966. p. 515-545.

6. Dickinson, S.M. The flexural vibration of rectangular orthotropic plates. Transactions of the American Society of Mechanical Engineers, Journal of Applied Mechanics 91:101-106. March, 1969.

7. Dong, S.B., K.S. Pister and R.L. Taylor. On the theory of laminated anisotropic shells and plates. Journal of the Aerospace Sciences 29:969-975. August, 1962.

8. Fox, R.L. and M.C. Kapoor. A minimization method for the solution of the eigenproblem arising in structural dynamics. In: Proceedings of the Second Conference on Matrix Methods in Structural Mechanics, Report no. AFFDL-TR-68-150, Wright-Patterson Air Force Base, 1969. p. 271-306.

9. Harper, F.C., W.J. Warlow and B.L. Clarke. The forces applied to the floor by the foot in walking: Part I. Walking on a level surface. London, Department of Scientific and Industrial Research, Building Research Station, 1961. 28 p. (Research paper 32).

10. Hearmon, R.F.S. The frequency of flexural vibration of rectangular orthotropic plates with clamped or supported edges. Transactions of the American Society of Mechanical Engineers, Journal of Applied Mechanics 81:537-540. December, 1959.

11. International Conference of Building Officials. Uniform building code. Pasadena, 1970. 651 p.

12. James, W.L. Effect of temperature and moisture content on internal friction and speed of sound in Douglas fir. Forest Products Journal 11:383-390. September, 1961.

13. Kuenzi, Edward W. and T.L. Wilkinson. Composite beams - effect of adhesive or fastener rigidity. Madison, U.S. Forest Products Laboratory, 1971. 22 p. (Research paper FPL 152).

14. Laursen, Harold I. Structural analysis. New York, McGraw-Hill, 1969. 496 p.

15. McGlenn, John and B.J. Hartz. Finite element analysis of plywood plates. Proceedings of the American Society of Civil Engineers, Journal of the Structural Division 94:551-563. February, 1968.

16. Pestel, Eduard C. Dynamic stiffness matrix formulation by means of Hermitian polynomials. In: Proceedings of the First Conference on Matrix Methods in Structural Mechanics, Report no. AFFDL-TR-66-80, Wright-Patterson Air Force Base, 1965. p. 479-502.

17. Polensek, Anton. Human response to vibration of wood-joist floor systems. Wood Science 3:111-119. October, 1970.

18. Polensek, Anton. Static and dynamic properties of glued wood-joist floors. Forest Products Journal 21(12):31-39. December, 1971.

19. Russel, William A. Deflection characteristics of residential wood-joist floor systems. Washington, D.C., U.S. Housing and Home Finance Agency, 1954. 64 p. (Housing research paper no. 30.)

20. Siess, Chester P., I.M. Viest, and N.M. Newmark. Studies of slab and beam highway bridges: Part III. Urbana, University of Illinois, The Engineering Experiment Station, February 1952. 11 p. (Bulletin 396).

21. Tezcan, Semih, S. Discussion of: Simplified formulation of stiffness matrices, by Peter M. Wright. Proceedings of the American Society of Civil Engineers, Journal of the Structural Division 89:445-449, December, 1963.

22. Timoshenko, S. and S. Woinowsky-Krieger. Theory of plates and shells. New York, McGraw-Hill, 1959. 580 p.

23. U.S. Forest Products Laboratory. Wood handbook. Madison, U.S. Department of Agriculture, 1955. 528 p. (Agriculture handbook no. 72.)

24. West Coast Lumbermen's Association. Standard grading and dressing rules. Portland, Oregon. 1969. 368 p. (No. 15, Revised January 1, 1969).

25. Wilkinson, Thomas Lee. Theoretical lateral resistance of nailed joints. Proceedings of the American Society of Civil Engineers, Journal of the Structural Division 97:1381-1398. May, 1971.

26. Yeh, Chi-Tung, B.J. Hartz, and C.B. Brown. Damping in glued and nailed wood structures. November, 1970. 41 p. (Report submitted to: U.S. Forest Service, Pacific Northwest Forest and Range Experiment Station, Seattle, Washington).

27. Zienkiewicz, O.C. and Y.K. Cheung. The finite element method in structural and continuum mechanics. London, McGraw-Hill, 1967. 274 p.

APPENDICES

APPENDIX A

FINITE ELEMENT MATRICES

Stiffness and mass matrices of the plate element are derived in this appendix. Stiffness and mass matrices of the beam element can be found in the literature (16), but are given herein for convenience. Because the uniform load is the most common load in floor design, a load matrix for this load is also included in this appendix.

A. 1. Derivation of Plate Element Matrices

The variables in Equation (2. 12) can be made dimensionless by letting

$$x = a\xi \tag{A.1}$$

and

$$y = b\eta \tag{A.2}$$

Substitution in Equation (2. 12) results in

$$-2\omega^2 \rho h_p ab \int_0^1 \int_0^1 w \frac{\partial w}{\partial g_m} d\xi d\eta + \int_0^1 \int_0^1 \left[\frac{bD_{11}}{a^3} w_{\xi\xi} \frac{\partial w_{\xi\xi}}{\partial g_m} \right.$$

$$\left. + \frac{D_{12}}{ab} \left(w_{\eta\eta} \frac{\partial w_{\xi\xi}}{\partial g_m} + w_{\xi\xi} \frac{\partial w_{\eta\eta}}{\partial g_m} \right) + \frac{aD_{22}}{b^3} w_{\eta\eta} \frac{\partial w_{\eta\eta}}{\partial g_m} + \frac{4D_{33}}{ab} w_{\xi\eta} \frac{\partial w_{\xi\eta}}{\partial g_m} \right] d\xi d\eta$$

$$+ i\omega cab \int_0^1 \int_0^1 w \frac{\partial w}{\partial g_m} d\xi d\eta = ab \int_0^1 \int_0^1 \frac{\partial W_e}{\partial g_m} d\xi d\eta \tag{A.3}$$

Displacement w in terms of the fourth order Hermitian polynomials (16) is

$$w = \{h(\xi)\}^T [W] \{h(\eta)\} \tag{A.4}$$

where

$$[W] = \begin{bmatrix} [W_i] & [W_j] \\ [W_\ell] & [W_k] \end{bmatrix} \tag{A.5}$$

$$[W_i] = \begin{bmatrix} w_i & w_{i,\eta} \\ w_{i,\xi} & w_{i,\xi\eta} \end{bmatrix} \tag{A.6}$$

$$\{h(\xi)\} = \begin{Bmatrix} h_1 \\ h_2 \\ h_3 \\ h_4 \end{Bmatrix} = \begin{Bmatrix} 1 - 3\xi^2 + 2\xi^3 \\ \xi - 2\xi^2 + \xi^3 \\ 3\xi^2 - 2\xi^3 \\ -\xi^2 + \xi^3 \end{Bmatrix} \tag{A.7}$$

and

$$\{h(\eta)\} = \begin{Bmatrix} \ell_1 \\ \ell_2 \\ \ell_3 \\ \ell_4 \end{Bmatrix} = \begin{Bmatrix} 1 - 3\eta^2 + 2\eta^3 \\ \eta - 2\eta^2 + \eta^3 \\ 3\eta^2 - 2\eta^3 \\ -\eta^2 + \eta^3 \end{Bmatrix} \tag{A.8}$$

Displacement w is transformed into a more workable form by letting

$$w = \{L\}^T [H] \{W\} \tag{A.9}$$

where

$$\{L\}^T = \{ \{L_1\}\{L_2\}\{L_3\}\{L_4\} \} \tag{A.10}$$

$$\{L_n\} = \{\ell_n \ell_n \ell_n \ell_n\} \tag{A.11}$$

$$\lceil H \rfloor = \begin{bmatrix} \lceil \bar{H} \rfloor & & & 0 \\ & \lceil \bar{H} \rfloor & & \\ & & \lceil \bar{H} \rfloor & \\ 0 & & & \lceil \bar{H} \rfloor \end{bmatrix} \tag{A.12}$$

$$\lceil \bar{H} \rfloor = \begin{bmatrix} h_1 & & & 0 \\ & h_2 & & \\ & & h_3 & \\ 0 & & & h_4 \end{bmatrix} \tag{A.13}$$

$$\{W\} = \begin{Bmatrix} \{W_i\} \\ \{W_j\} \\ \{W_\ell\} \\ \{W_k\} \end{Bmatrix} \tag{A.14}$$

$$\{W_i\} = \begin{Bmatrix} w_i \\ w_{i,\eta} \\ w_{i,\xi} \\ w_{i,\xi\eta} \end{Bmatrix} \tag{A.15}$$

The nodal displacements contained in the displacement vector $\{w\}$ of Equation (2.13), also are the generalized coordinates g_m in Equation (A.3).

Partial derivatives of $\{w\}$ now can easily be determined

$$w_{\xi\xi} = \{L\}^T \lceil H \rfloor_{\xi\xi} \{W\} \tag{A.16}$$

$$w_{\eta\eta} = \{L\}^T_{\eta\eta} \lceil H \rfloor \{W\} \tag{A.17}$$

$$w_{\xi\eta} = \{L\}^T_{\eta} \lceil H \rfloor_{\xi} \{W\} \tag{A.18}$$

Partial differentiation of Equation (A.9), (A.16), (A.17) and (A.18) with respect to g_m involves the differentiation of $\{W\}$ only. If g_m is the element of the m-th row in $\{w\}$, the derivative with respect to g_m gives a vector with all the elements but that of the m-th row equal to zero. The m-th row of this matrix is 1, b, a and ab corresponding to w, w_y, w_x and w_{xy} of the m-th row in $\{w\}$.[2/] Therefore,

$$\partial w_{\xi\xi} / \partial g_m = \ell_m h_{m,\xi\xi} s_m \tag{A.19}$$

where

s_m - equals to 1, b, a or ab

$$\partial w_{\eta\eta} / \partial g_m = \ell_{m,\eta\eta} h_m s_m \tag{A.20}$$

$$\partial w_{\xi\eta} / \partial g_m = \ell_{m,\eta} h_{m,\xi} s_m \tag{A.21}$$

$$\partial w / \partial g_m = \ell_m h_m s_m \tag{A.22}$$

[2/] Note that $\dfrac{\partial w_\eta}{\partial w_y} = \dfrac{\partial w_\eta}{\partial [\partial w / \partial (b\eta)]} = \dfrac{\partial w_\eta}{\partial w_\eta / b} = b$ etc.

Equations (A. 9) and (A. 16) through (A. 22) are substituted into Equation (A. 3) and rearranged to obtain

$$\frac{s_m}{ab}\Big\langle -2\omega^2\rho h_p a^2 b^2 \int_0^1 \ell_m \{L\}^T d\eta \int_0^1 h_m \lceil H \rfloor d\xi$$

$$+ p^{-2} D_{11} \int_0^1 \ell_m \{L\}^T d\eta \int_0^1 h_{m,\xi\xi} \lceil H \rfloor_{\xi\xi} d\eta$$

$$+ D_{12}\left(\int_0^1 \ell_m \{L_{\eta\eta}\} d\eta \int_0^1 h_{m,\xi\xi} \lceil H \rfloor d\xi + \int_0^1 \ell_{m,\eta\eta} \{L\}^T d\eta \int_0^1 h_m \lceil H \rfloor_{\xi\xi} d\xi\right)$$

$$+ p^2 D_{22} \int_0^1 \ell_{m,\eta\eta} \{L\}^T_{\eta\eta} d\eta \int_0^1 h_m \lceil H \rfloor d\xi + 4D_{33} \int_0^1 \ell_{m,\eta} \{L\}^T_{\eta} d\eta \int_0^1 h_{m,\xi} \lceil H \rfloor_{\xi} d\xi$$

$$+ i\omega c a^2 b^2 \int_0^1 \ell_m \{L\}^T d\eta \int_0^1 h_m \lceil H \rfloor d\xi \Big\rangle = ab Q_m \qquad \text{(A. 23)}$$

The terms in the sum on the left side of Equation (A. 23) give the m-th row of the plate element matrices. The first term belongs to the mass matrix, the next four terms are part of the stiffness matrix, and the last term corresponds to the damping matrix. The integrands in Equation (A. 23) are the fourth order Hermitian polynomials and their derivatives. The integration, simple but cumbersome, was performed using an electronic desk calculator. A computer solution would have been more appropriate and not very difficult because of the matrix nature of Equation (A. 23).

Equation (A. 23) was evaluated for all of the elements of vector {w} and the results were expressed in a matrix form to give

$$\frac{1}{30ab}\lceil L\rfloor\left\langle \omega^2 \frac{\rho h_p a^2 b^2}{5880}[\bar{M}] + \frac{\bar{p}^{-2}}{7} D_{11}[K_1] + \frac{1}{15} D_{12}[K_2] \right.$$

$$\left. + \frac{p^2}{7} D_{22}[K_3] + \frac{1}{30} D_{33}[K_4] + i\omega \frac{a^2 b^2 c}{11760}[\bar{M}] \right\rangle \lceil L\rfloor\{w\} = ab\{P\} \tag{A.24}$$

where

$$\lceil L\rfloor = \begin{bmatrix} \lceil\bar{L}\rfloor & & & 0 \\ & \lceil\bar{L}\rfloor & & \\ & & \lceil\bar{L}\rfloor & \\ 0 & & & \lceil\bar{L}\rfloor \end{bmatrix} \tag{A.25}$$

$$\lceil\bar{L}\rfloor = \begin{bmatrix} 1 & & & 0 \\ & b & & \\ & & a & \\ 0 & & & ab \end{bmatrix} \tag{A.26}$$

$$[K_1] = \begin{bmatrix}
936 & 132 & 468 & 66 & 324 & -78 & 162 & -39 & -936 & -132 & 468 & 66 & -324 & 78 & 162 & -39 \\
 & 24 & 66 & 12 & 78 & -18 & 39 & -9 & -132 & -24 & 24 & 12 & -78 & 18 & 39 & -9 \\
 & & 312 & 44 & 162 & -39 & 108 & -26 & -468 & -66 & 156 & 22 & -162 & 39 & 54 & -13 \\
 & & & 8 & 39 & -9 & 26 & -6 & -66 & -12 & 22 & 4 & -39 & 9 & 13 & -3 \\
 & & & & 936 & -132 & 468 & -66 & -324 & -78 & 162 & 39 & -936 & 132 & 468 & -66 \\
 & & & & & 24 & -66 & 12 & 78 & 18 & -39 & -9 & 132 & -24 & -66 & 12 \\
 & & & & & & 312 & -44 & -162 & -39 & 54 & 13 & -468 & 66 & 156 & -22 \\
 & & & & & & & 8 & 39 & 9 & -13 & -3 & 66 & -12 & -22 & 4 \\
 & & & & & & & & 936 & 132 & -468 & -66 & 324 & -78 & -162 & 39 \\
 & & & & & & & & & 24 & -66 & -12 & 78 & -18 & -39 & 9 \\
 & & & & & & & & & & 312 & 44 & -162 & 39 & 108 & -26 \\
 & & & & & & & & & & & 8 & -39 & 9 & 26 & -6 \\
 & & & & & & & & & & & & 936 & -132 & -468 & 66 \\
 & & & & & & & & & & & & & 24 & 66 & -12 \\
 & & & & & & & & & & & & & & 312 & -44 \\
 & & & & & & & & & & & & & & & 8
\end{bmatrix} \qquad \text{(A.27)}$$

Symmetry

$$[K_2] = \begin{bmatrix}
1296 & 648 & 648 & 99 & -1296 & 108 & -648 & 54 & -1296 & -648 & 108 & 54 & 1296 & -108 & -108 & 9 \\
 & 144 & 549 & 72 & -108 & -36 & -54 & -18 & -648 & -144 & 54 & 12 & 108 & 36 & -9 & -3 \\
 & & 144 & 72 & -648 & 54 & -144 & 12 & -108 & -54 & -36 & -18 & 108 & -9 & 36 & -3 \\
 & & & 16 & -54 & -18 & -12 & -4 & -54 & -12 & -18 & -4 & 9 & 3 & 3 & 1 \\
 & & & & 1296 & -648 & 648 & -99 & 1296 & 108 & -108 & -9 & -1296 & 648 & 108 & -54 \\
 & & & & & 144 & -549 & 72 & -108 & 36 & 9 & -3 & 648 & -144 & -54 & 12 \\
 & & & & & & 144 & -72 & 108 & 9 & 36 & 3 & -108 & 54 & -36 & 18 \\
 & & & & & & & 16 & -9 & 3 & -3 & 1 & 54 & -12 & 18 & -4 \\
 & & & & & & & & 1296 & 648 & -648 & -99 & -1296 & 108 & 648 & -54 \\
 & & & & & & & & & 144 & -549 & -72 & -108 & -36 & 54 & 18 \\
 & & & & & & & & & & 144 & 72 & 648 & -54 & -144 & 12 \\
 & & & & & & & & & & & 16 & 54 & 18 & -12 & -4 \\
 & & & & & & & & & & & & 1296 & -648 & -648 & 99 \\
 & & & & & & & & & & & & & 144 & 549 & -72 \\
 & & & & & & & & & & & & & & 144 & -72 \\
 & & & & & & & & & & & & & & & 16
\end{bmatrix}$$

Symmetry

(A. 28)

$$[K_3] = \begin{bmatrix}
936 & 468 & 132 & 66 & -936 & 468 & -132 & 66 & 324 & 162 & -78 & -39 & -324 & 162 & 78 & -39 \\
 & 312 & 66 & 44 & -468 & 156 & -66 & 22 & 162 & 108 & -39 & -26 & -162 & 54 & 39 & -13 \\
 & & 24 & 12 & -132 & 66 & -24 & 12 & 78 & 39 & -18 & -9 & -78 & 39 & 18 & -9 \\
 & & & 8 & -66 & 22 & -12 & 4 & 39 & 26 & -9 & -6 & -39 & 13 & 9 & -3 \\
 & & & & 936 & -468 & 132 & -66 & -324 & -162 & 78 & 39 & 324 & -162 & -78 & 39 \\
 & & & & & 312 & -66 & 44 & 162 & 54 & -39 & -13 & -162 & 108 & 39 & -26 \\
 & & & & & & 24 & -12 & -78 & -39 & 18 & 9 & 78 & -39 & -18 & 9 \\
 & & & & & & & 8 & 39 & 13 & -9 & -3 & -39 & 26 & 9 & -6 \\
 & & & & & & & & 936 & 468 & -132 & -66 & -936 & 468 & 132 & -66 \\
 & & & & & & & & & 312 & -66 & -44 & -468 & 156 & 66 & -22 \\
 & & & & & & & & & & 24 & 12 & 132 & -66 & -24 & 12 \\
 & & & & & & & & & & & 8 & 66 & -22 & -12 & 4 \\
 & & & & & & & & & & & & 936 & -468 & -132 & 66 \\
 & & & & & & & & & & & & & 312 & 66 & -44 \\
 & & & & & & & & & & & & & & 24 & -12 \\
 & & & & & & & & & & & & & & & 8
\end{bmatrix}$$

Symmetry

(A.29)

$$[K_4] = \begin{bmatrix}
1296 & 108 & 108 & 9 & -1296 & 108 & -108 & 9 & -1296 & -108 & 108 & 9 & 1296 & -108 & -108 & 9 \\
 & 144 & 9 & 12 & -108 & -36 & -9 & -3 & -108 & -144 & 9 & 12 & 108 & 36 & -9 & -3 \\
 & & 144 & 12 & -108 & 9 & -144 & 12 & -108 & -9 & -36 & -3 & 108 & -9 & 36 & -3 \\
 & & & 16 & -9 & -3 & -12 & -4 & -9 & -12 & -3 & -4 & 9 & 3 & 3 & 1 \\
 & & & & 1296 & -108 & 108 & -9 & 1296 & 108 & -108 & -9 & -1296 & 108 & 108 & -9 \\
 & & & & & 144 & -9 & 12 & -108 & 36 & 9 & -3 & 108 & -144 & -9 & 12 \\
 & & & & & & 144 & -12 & 108 & 9 & 36 & 3 & -108 & 9 & -36 & 3 \\
 & & & & & & & 16 & -9 & 3 & -3 & 1 & 9 & -12 & 3 & -4 \\
 & & & & & & & & 1296 & 108 & -108 & -9 & -1296 & 108 & 108 & -9 \\
 & & & & & & & & & 144 & -9 & -12 & -108 & -36 & 9 & 3 \\
 & & & & & & & & & & 144 & 12 & 108 & -9 & -144 & 12 \\
 & & & & & & & & & & & 16 & 9 & 3 & -12 & -4 \\
 & & & & & & & & & & & & 1296 & -108 & -108 & 9 \\
 & & & & & & & & & & & & & 144 & 9 & -12 \\
 & & & & & & & & & & & & & & 144 & -12 \\
 & & & & & & & & & & & & & & & 16
\end{bmatrix}$$

Symmetry

(A. 30)

$$[\overline{M}] = \begin{bmatrix}
24336 & 3432 & 3432 & 484 & 8424 & -2028 & 1188 & -286 & 8424 & 1188 & -2028 & -286 & 2916 & -702 & -702 & 169 \\
 & 624 & 484 & 88 & 2028 & -468 & 286 & -66 & 1188 & 216 & -286 & -52 & 702 & -162 & -169 & 39 \\
 & & 624 & 88 & 1188 & -286 & 216 & -52 & 2028 & 286 & -468 & -66 & 702 & -169 & -162 & 39 \\
 & & & 16 & 286 & -66 & 52 & -12 & 286 & 52 & -66 & -12 & 169 & -39 & -39 & 9 \\
 & & & & 24336 & -3432 & 3432 & -484 & 2916 & 702 & -702 & -169 & 8424 & -1188 & -2028 & 286 \\
 & & & & & 624 & -484 & 88 & -702 & -162 & 169 & 39 & -1188 & 216 & 286 & -52 \\
 & & & & & & 624 & -88 & 702 & 169 & -162 & -39 & 2028 & -286 & -468 & 66 \\
 & & & & & & & 16 & -169 & -39 & 39 & 9 & -286 & 52 & 66 & -12 \\
 & & & & & & & & 24336 & 3432 & -3432 & -484 & 8424 & -2028 & -1188 & 286 \\
 & & & & & & & & & 624 & -484 & -88 & 2028 & -468 & -286 & 66 \\
 & & & & & & & & & & 624 & 88 & -1188 & 286 & 216 & -52 \\
 & & & & & & & & & & & 16 & -286 & 66 & 52 & -12 \\
 & & & & & & & & & & & & 24336 & -3432 & -3432 & 484 \\
 & & & & & & & & & & & & & 624 & 484 & -88 \\
 & & & & & & & & & & & & & & 624 & -88 \\
 & & & & & & & & & & & & & & & 16
\end{bmatrix}$$

Symmetry

(A.31)

The stiffness matrix is defined by Equation (2.15), using $\lceil L \rfloor$, $[K_1]$, $[K_2]$, $[K_3]$, and $[K_4]$. The mass matrix is defined by Equation (2.16) using $\lceil L \rfloor$ and $[\overline{M}]$. The damping matrix is defined by Equation (2.14) using the mass matrix.

With a minor modification, the above stated procedure can be used to develop the element matrices for other types of displacement functions. A computer program, if developed, can offer a quick solution for higher order polynomials.

A.2. Beam Element Matrices

$$\lceil L_b \rfloor = \begin{bmatrix} 1 & 0 & 0 & 0 \\ 0 & a & 0 & 0 \\ 0 & 0 & 1 & 0 \\ 0 & 0 & 0 & a \end{bmatrix} \tag{A.32}$$

$$[K_b] = \begin{bmatrix} 12 & 6 & -12 & 6 \\ 6 & 4 & -6 & 2 \\ -12 & -6 & 12 & -6 \\ 6 & 2 & -6 & 4 \end{bmatrix} \tag{A.33}$$

$$[\overline{M}_b] = \frac{1}{420} \begin{bmatrix} 156 & 22 & 54 & -13 \\ 22 & 4 & 13 & -3 \\ 54 & 13 & 156 & -22 \\ -13 & -3 & -22 & 4 \end{bmatrix} \tag{A.34}$$

A.3. Distributed Load Vectors

$$\{Q\} = ab\lceil L \rfloor \int_0^1 \int_0^1 p(\xi, \eta) \begin{Bmatrix} \ell_1 h_1 \\ \ell_2 h_1 \\ \ell_1 h_2 \\ \ell_2 h_2 \\ \ell_3 h_1 \\ \ell_4 h_1 \\ \ell_3 h_2 \\ \ell_4 h_2 \\ \ell_1 h_3 \\ \ell_2 h_3 \\ \ell_1 h_4 \\ \ell_2 h_4 \\ \ell_3 h_3 \\ \ell_4 h_3 \\ \ell_3 h_4 \\ \ell_4 h_4 \end{Bmatrix} d\xi d\eta = \frac{abp}{144} \lceil L \rfloor \begin{Bmatrix} 36 \\ 6 \\ 6 \\ 1 \\ 36 \\ -6 \\ 6 \\ -1 \\ 36 \\ 6 \\ -6 \\ -1 \\ 36 \\ -6 \\ -6 \\ 1 \end{Bmatrix} \qquad \text{(A.35)}$$

The vector on the far right is obtained by evaluating the double integral for a constant uniform load p.

APPENDIX B

THE COMPUTER PROGRAM

The computer program is composed of three individual programs written in Fortran IV. The first one, STIMASLO, forms the stiffness, mass and load matrix of the floor and stores them in two sequential disk storage areas. The second program, NATFREQ, solves for the modal frequencies and corresponding modal vectors using the stiffness and mass matrix from one of the sequential disk storage areas. The third program, STREDISP, performs static displacement analysis and dynamic response analysis using the stiffness, mass and load matrix from the remaining sequential disk storage area. A brief description of each of these programs and the program listings are given in this appendix.

Program STIMASLO forms the stiffness, mass and load matrices of the plate bending element and the T-beam element and combines them into the system matrices. The program has several built-in options as to the type of analysis to be performed, type of loading applied and the choice between the matrices for the floor and orthotropic plate.

Program NATFREQ uses two subroutines, NROOT and EIGEN. Subroutine NROOT, given in the program listing, calculates the eigenvalues and the corresponding eigenvectors of a real

non-symmetric dynamic stiffness matrix $[D_s]$ defined as $[M_s]^{-1}[K_s]$, where $[M_s]$ and $[K_s]$ are real symmetric matrices and $[M]$ also is positive-definite. Subroutine NROOT calls for subroutine EIGEN which computes the eigenvalues and eigenvectors of a real symmetric matrix. Subroutine EIGEN, not included in the computer listing, is available to all users in the Oregon State University Computer Center Program Library.

Program STREDISP uses five subroutines; STRESS, OUTPUT1, OUTPUT2, NUMINT and MATINV. The main program has several options which direct the flow, permitting the execution of only those statements which are necessary for the chosen analysis. The choices are between static displacement analysis and dynamic response analysis, joist floors and orthotropic plates, uniform load and concentrated loads, and initial displacement and numerically defined loading function as a vibration impulse. Subroutine STRESS calculates stresses in outer layers of the joists and floor covering. Subroutines OUTPUT1 and OUTPUT2 print stresses and displacements, respectively, for static displacement analysis and dynamic response analysis. Subroutine NUMINT, the core for dynamic response analysis, numerically integrates equations of motion using the linear acceleration method. Finally, subroutine MATINV is a standard matrix inversion subroutine, known as Jordan's method, which is used to solve the system of simultaneous linear equations.

Program EIGENV[3/] with subroutines KXMX, FBMIN2, FANDG, PROD and INGEN can be used for frequency analysis instead of NATFREQ. The program, based on an iterative procedure, calculates the desired number of the lowest modal frequencies and eigenvectors, and requires initial estimates for the eigenvectors.

[3/] This program, supplied by Dr. R. L. Fox of Case Western Reserve University, was adapted for OS-3, the computer system operated by the Oregon State University Computer Center.

```
      PROGRAM STIMASLO
C THIS PROGRAM FORMS STIFFNESS AND CONSISTENT MASS MATRICES
C OF JOIST FLOOR WITH MUILTILAYERED FLOOR COVERING
      DIMENSION HP(9),XK1(16,16),XK2(16,16),XK3(16,16),XK4(16,16)
     1,XM(16,16),W(20),H(20),XE(20),XKB(4,4),XMB(4,4),KP(30,16),
     2KJ(30,4),YK(60,60),YM(60,60),QU(16),Q(60),QS(4),ST(20)
     3,EX(20),IX(35),DELK(20)
  798 FORMAT(1X,6E11.4)
  300 FORMAT(1X,20I3)
  302 FORMAT(1X,2F8.4,I3,2F10.0,3F7.4)
      DO 702 I=1,16
      DO 706 J=I,16
  706 XK1(I,J)=FFIN(2)
      DO 707 J=I,16
  707 XK2(I,J)=FFIN(2)
      DO 708 J=I,16
  708 XK3(I,J)=FFIN(2)
      DO 702 J=I,16
  702 XK4(I,J)=FFIN(2)
      DO 709 I=1,16
      DO 709 J=I,16
      XM(I,J)=FFIN(2)
  709 XM(J,I)=XM(I,J)
      DO 710 I=1,4
      DO 711 J=I,4
      XKB(I,J)=FFIN(2)
  711 XKB(J,I)=XKB(I,J)
      DO 710 J=1,4
      XMB(I,J)=FFIN(2)
  710 XMB(J,I)=XMB(I,J)
      DO 201 I=1,16
  201 QU(I)=FFIN(2)
      DO 203 I=1,4
  203 QS(I)=FFIN(2)
      KOPT = FFIN(1)
      LOPT=FFIN(1)
      NOPT=FFIN(1)
      KL=FFIN(1)
      IOP=FFIN(1)
      JOP=FFIN(1)
      IFRQ=FFIN(1)
      IMAS=FFIN(1)
C OPTIONS: KOPT=1 DYNAMIC RESPONSE ANALYSIS, LOPT=0 CONCENTR.
C          LOADS, NOPT=1 STATIC DISPLACEMENT ANALYSIS,
C          KL=0 OTRHOTROPIC PLATE ANALYSIS, IOP=0 EDGE AT Y=0
C          SUPPORTED ALONG ITS LENGTH (UNSUPP.:IOP=1), JOP=0
C          EDGE AT Y=L SUPP. ALONG ITS LENGTH (UNSUPP.: JOP=1)
C          IFRQ=1 FILE IN LUN 7 FOR FREQUENCY ANALYSIS
C          IMAS=0 SELF-WEIGHT OF FLOOR NOT INCLUDED IN LOADING
      EL =FFIN(1)
      ET = FFIN(1)
      G = FFIN(1)
      PTL = FFIN(1)
      PLT = FFIN(1)
      NP = FFIN(1)
C GRAIN ORIENTATION OF TOP LAYER (NP=1) IS IN Y-DIRECTION (ACROSS
C THE SPAN)
      NPP = (NP+1)/2
      DO 700 I=1,NPP
  700 HP(I) = FFIN(1)
      SUMA = 0.0
      SUMH = 0.0
      DO 701 I=1,NPP
      IS = (-1)**I
      SUMA = SUMA - IS*HP(I)
  701 SUMH = SUMH - IS*(HP(I)**3)
      PF = 2/(3*(1-PTL*PLT))
      HP1 = HP(1)**3
      D11 = PF*(SUMH*(ET-EL)+EL*HP1)
      D22 = PF*(SUMH*(EL-ET)+ET*HP1)
      D12 = PF*(SUMH*(ET*PLT-EL*PTL)+EL*PTL*HP1)
      A11 = 3*PF*(SUMA*(ET-EL)+EL*HP(1))
      D33 = 2*HP1*G/3
      A = FFIN(1)
      B = FFIN(1)
      P2 = A*A/(B*B)
      D11 = D11/(7.*P2)
      D12 = D12/15.
      D22 = D22*P2/7.
      D33 = D33/7.S
      DO 703 I=1,16
      DO 703 J=I,16
      XK1(I,J)=D11*XK1(I,J)+D12*XK2(I,J)+D22*XK3(I,J)+D33*XK4(I,J)
  703 XK1(J,I)=XK1(I,J)
      P2 = 30.*A*B
      PMAS=FFIN(1)
C PMAS=MASS PER SQUARE INCH OF FLOOR COVERING
      P1=I76400./(A*B*PMAS)
      DO 704 I=1,16
      IF(I.EQ.1.OR.I.EQ.S.OR.I.EQ.9.OR.I.EQ.13) X=1.
      IF(I.EQ.2.OR.I.EQ.6.OR.I.EQ.10.OR.I.EQ.14) X=B
      IF(I.EQ.3.OR.I.EQ.7.OR.I.EQ.11.OR.I.EQ.15) X=A
      IF(I.EQ.4.OR.I.EQ.8.OR.I.EQ.12.OR.I.EQ.16) X=A*B
      QU(I)=X*QU(I)
      DO 704 J=1,16
      XK1(I,J)=X*XK1(I,J)
      XK1(J,I)=X*XK1(J,I)/P2
      IF(.NOT.KOPT.EQ.1) GO TO 704
      XM(I,J)=X*XM(I,J)
      XM(J,I)=X*XM(J,I)/P1
  704 CONTINUE
      NBB=FFIN(1)
      NBP=FFIN(1)
C NBB,NBP ARE NUMBER OF PLATE ELEMENTS ALONG X-AXIS AND/OR Y-AXIS
      NB=NBP+1
      IF(KL.EQ.0) GO TO 760
      P1=A/420.
      P2=A**3
      DO 717 I=1,4
      IF(I.EQ.1.OR.I.EQ.3) X=1.
      IF(I.EQ.2.OR.I.EQ.4) X=A
      QS(I)=QS(I)*X*A/12.
      DO 717 J=1,4
      XKB(I,J)=X*XKB(I,J)/P2
      XKB(J,I)=XKB(J,I)*X
      IF(.NOT.KOPT.EQ.1) GO TO 717
      XMB(I,J)=XMB(I,J)*X*P1
      XMB(J,I)=XMB(J,I)*X
  717 CONTINUE
      DO 712 I=1,NB
  712 XE(I)=FFIN(1)
      DO 714 I=1,NB
  714 W(I)=FFIN(1)
      DO 715 I=1,NB
  715 H(I)=FFIN(1)
      BRE=FFIN(1)
      DO 719 I=1,NB
  719 DELK(I)=FFIN(1)
C XE-MODULI OF ELASTICITY,W-WIDTHS,AND H-HEIGHTS OF JOISTS
C BRE IS EFFECTIVE WIDTH OF FLANGE OF FLOOR COVERING, DELK ARE
C STIFFNESS REDUCTION RATIOS DUE TO SLIP IN JOIST-SUBFLOOR JOINTS
      P2=2.*HP(1)
      DO 716 I=1,NB
      P1=BRE*A11
      IF(I.EQ.1.OR.I.EQ.NB) P1=P1/2.
      W(I)=W(I)*H(I)*XE(I)
      EX(I)=(P2+H(I))/(2.*(W(I)/P1+1.))
      ST(I)=XE(I)*(H(I)/2.+EX(I))/DELK(I)
      EX(I)=H(I)/2.-EX(I)+HP(1)
  716 XE(I)=(W(I)*H(I)*H(I)/12.+((H(I)+P2)*(H(I)+P2)*P1/
     1(4.+4.*P1/W(I))))/DELK(I)
      DO 713 I=1,NB
```

```
      H(I)=FFIN(1)
  713 XK1(I)=H(I)
      NFB=NB*NBB
  760 N=FFIN(1)
C H - MASS PER INCH OF JOIST LENGHT,LB*SEC**2 PER INCH**2
C N - SYSTEM MATRIX SIZE
      NFP=NBP*NBB
C KP-KODE NUMBERS FOR PLATE, KJ-KODE NUMBERS FOR BEAMS
      DO 720 I=1,NFP
      DO 720 J=1,16
  720 KP(I,J)=FFIN(1)
      IF(KL.EQ.0) GO TO 775
      IK=1
      DO 721 I=1,NFB
      DO 721 J=1,4
      KJ(I,J)=FFIN(1)
      IJ=KJ(I,J)
      IF(IJ.EQ.0) GO TO 721
      JK=IK-1
      DO 740 K=1,JK
      IF(IX(K)-IJ) 740,721,740
  740 CONTINUE
      IX(IK)=IJ
      IK=IK+1
  721 CONTINUE
  775 IF(.NOT.NOPT.EQ.1) GO TO 761
      UN=FFIN(1)
      IF(IMAS.EQ.0) PMAS=0.
C  UN = UNIFORM LOAD PER SQUARE FOOT OF FLOOR AREA
      UL=A*B*(UN+55593.2*PMAS)/20736.
  761 DO 722 I=1,NFP
      DO 722 J=1,16
      IF(.NOT.NOPT.EQ.1) GO TO 266
      KAJ=KP(I,J)
      IF(KAJ.EQ.0) GO TO 722
      Q(KAJ)=Q(KAJ)+UL*QU(J)
  266 DO 722 L=J,16
      KA=KP(I,J)
      KB=KP(I,L)
      IF(KA.EQ.0.OR.KB.EQ.0) GO TO 722
      IF(KA.LE.KB) GO TO 723
      MA=KA
      KA=KB
      KB=MA
  723 YK(KA,KB)=YK(KA,KB)+XK1(J,L)
      IF(.NOT.KOPT.EQ.1) GO TO 722
      YM(KA,KB)=YM(KA,KB)+XM(J,L)
  722 CONTINUE
      IF(KL.EQ.0) GO TO 730
      DO 724 I=1,NFB
      IF(I.LE.NBB) GO TO 726
      M=((I-1)/NBB)+1
      GO TO 727
  726 M=1
  727 DO 724 J=1,4
      IF(.NOT.NOPT.EQ.1) GO TO 276
      KAB=KJ(I,J)
      IF(KAB.EQ.0) GO TO 724
      IF(IMAS.EQ.0) XK1(M)=0.
      Q(KAB)=Q(KAB)+386.06*XK1(M)*QS(J)
  276 DO 724 L=J,4
      KA=KJ(I,J)
      KB=KJ(I,L)
      IF(KA.EQ.0.OR.KB.EQ.0) GO TO 724
      IF(KA.LE.KB) GO TO 725
      MA=KA
      KA=KB
      KB=MA
  725 YK(KA,KB)=YK(KA,KB)+XE(M)*XKB(J,L)
      IF(.NOT.KOPT.EQ.1) GO TO 724
      YM(KA,KB)=YM(KA,KB)+H(M)*XMB(J,L)
  724 CONTINUE
  730 DO 751 I=1,N
      DO 751 J=I,N
      YK(J,I)=YK(I,J)
      IF(.NOT.KOPT.EQ.1) GO TO 751
      YM(J,I)=YM(I,J)
  751 CONTINUE
      IF(.NOT.NOPT.EQ.1.OR.LOPT.EQ.1) GO TO 251
      NL=FFIN(1)
      DO 221 I=1,NL
      ND=FFIN(1)
  221 Q(ND)=Q(ND)+FFIN(1)
C  NL=NUMBER OF CONCENTRATED LOADS, NL=0 NO CONC. LOADS
C  ND= SYSTEM DISPLACEMENT NUMBER, Q(ND)=CONC. LOAD IN LBS.
  251 IF(.NOT.IFRQ.EQ.1) GO TO 80
      WRITE(7,308) N
      WRITE(7,798)((YK(I,J),YM(I,J),J=1,N),I=1,N)
      ENDFILE 7
      IF(IFRQ.EQ.1) GO TO 90
   80 WRITE(6,308) N
      DO 785 I=1,N
  785 WRITE(6,798)(YK(I,J),YM(I,J),J=1,N)
      WRITE(6,798)(Q(I),I=1,N)
      WRITE(6,302) A,B,KL,EL,ET,PTL,PLT,HP(1)
      WRITE(6,308) NB,NBB,IOP,JOP,KOPT,NOPT
      IF(KL.EQ.0) GO TO 99
      IK=IK-1
      WRITE(6,308) IK
      WRITE(6,308) (IX(I),I=1,IK)
      WRITE(6,798) (ST(I),EX(I),I=1,NB)
   99 ENDFILE 6
   90 CONTINUE
      END
```

```
      PROGRAM NATFREQ
C     COMPUTES EIGENVALUES AND EIGENVECTORS
C     MATRIX M AND/OR K  IS SYMMETRIC AND REAL POSITIVE
      DIMENSION STF(2500),SMS(2500),EIGVAL(50),EIGVEC(2500)
  300 FORMAT(1X,20I3)
  301 FORMAT(1X,6E11.4)
      READ(7,300) N
      NN=N*N
      READ(7,301) (STF(I),SMS(I),I=1,NN)
      CALL NROOT(N,STF,SMS,EIGVAL,EIGVEC)
      DO 75 I=1,N
   75 EIGVAL(I)=SQRT(EIGVAL(I))/6.28318
      WRITE(5,50)
   50 FORMAT(1X,'EIGENVALUES ARE'/)
      WRITE(5,60)(EIGVAL(I),I=1,N)
   60 FORMAT(1X,5E13.5)
      WRITE(5,70)
   70 FORMAT(1X,'EIGENVECTORS, IN THE SAME ORDER AS EIGENVALUES'/)
      WRITE(5,60)(EIGVEC(I),I=1,NN)
      END

      SUBROUTINE NROOT(M,A,B,XL,X)
C     COMPUTES EIGEN- VALUES AND VECTORS FOR B**-1*A=LAMBDA*X
      DIMENSION A(1),B(1),XL(1),X(1)
      K=1
      DO 100 J=2,M
```

```
      L=M*(J-1)
      DO 100 I=1,J
      L=L+1
      K=K+1
  100 B(K)=B(L)
      MV=0
      CALL EIGEN (B,X,M,MV)
      L=0
      DO 110 J=1,M
      L=L+J
  110 XL(J)=1.0/SQRT(ABS(B(L)))
      K=0
      DO 115 J=1,M
      DO 115 I=1,M
      K=K+1
  115 B(K)=X(K)*XL(J)
      DO 120 I=1,M
      N2=0
      DO 120 J=1,M
      N1=M*(I-1)
      L=M*(J-1)+I
      X(L)=0.0
      DO 120 K=1,M
      N1=N1+1
      N2=N2+1
  120 X(L)=X(L)+B(N1)*A(N2)
      L=0
      DO 130 J=1,M
      DO 130 I=1,J
      N1=I-M
      N2=M*(J-1)
      L=L+1
      A(L)=0.0
      DO 130 K=1,M
      N1=N1+M
      N2=N2+1
  130 A(L)=A(L)+X(N1)*B(N2)
      CALL EIGEN (A,X,M,MV)
      L=0
      DO 140 I=1,M
      L=L+I
  140 XL(I)=A(L)
      DO 150 I=1,M
      N2=0
      DO 150 J=1,M
      N1=I-M
      L=M*(J-1)+I
      A(L)=0.0
      DO 150 K=1,M
      N1=N1+M
      N2=N2+1
  150 A(L)=A(L)+B(N1)*X(N2)
      L=0
      K=0
      DO 180 J=1,M
      SUMV=0.0
      DO 170 I=1,M
      L=L+1
  170 SUMV=SUMV+A(L)*A(L)
      SUMV= SQRT(SUMV)
      DO 180 I=1,M
      K=K+1
  180 X(K)=A(K)/SUMV
      RETURN
      END
```

```
      PROGRAM STREDISP
C  THIS PROGRAM COMPUTES MAXIMUM DEFLECTIONS AND STRESSES
C  UNDER STATIC AND DYNAMIC LOADS
      COMMON/DATA/EL,ET,A,B,H1,IOPT,JOPT,N1,N2,NBB,PTL,PLT,NS,KL
      COMMON YQ(60,60),YK(60,60),YM(60,60),PT(700),D(60),
     1IX(30),JX(20),P(60),ST(20),EX(20),STX(20),STY(20)
      DIMENSION OM(20),PF(40)
  400 FORMAT(1X,6E11.4)
  403 FORMAT(1X,2F8.4,I3,2F10.0,3F7.4)
  404 FORMAT(1X,'STATIC ANALYSIS'//1X,'DISPLACEMENTS ARE,'
     1,1X,'INCHES AND/OR RADIANTS')
  406 FORMAT(1X/1X,'PLATE STRESSES S AT ND, Y-DIRECTION, PSI')
  407 FORMAT(1X/1X,'PLATE STRESSES S AT ND, X-DIRECTION, PSI')
  408 FORMAT(1X/1X,'JOIST STRESSES S AT ND, X-DIRECTION, PSI')
  409 FORMAT(1X,20I3)
  410 FORMAT(1X/1X,'DYNAMIC LOAD IS APPLIED AT DISP. NO.',I4)
  411 FORMAT(1X//1X,'DYNAMIC RESPONSE ANALYSIS')
  412 FORMAT(1X/1X,'VIBRATION STARTED BY INITIAL DISPLACEMENT')
      READ(6,409) N
      DO 1 I=1,N
    1 READ(6,400)(YK(I,J),YM(I,J),J=1,N)
      READ(6,400)(P(I),I=1,N)
      READ(6,403) A,B,KL,EL,ET,PTL,PLT,H1
      READ(6,409) NB,NBB,IOPT,JOPT,KOPT,NOPT
      IF(KL.EQ.0) GO TO 3
      READ(6,409) IK
      READ(6,409) (IX(I),I=1,IK)
      READ(6,400)(ST(I),EX(I),I=1,NB)
    3 EL=EL/(1.-PTL*PLT)
      ET=ET/(1.-PLT*PTL)
      NS=NB
      IF(IOPT.EQ.0.OR.JOPT.EQ.0) NS=NB-1
      IF(IOPT.EQ.0.AND.JOPT.EQ.0) NS=NB-2
      N1=2*(NBB+1)-3
      IF(IOPT.EQ.0.AND.JOPT.EQ.0) N1=2*(NBB+1)-2
      N2=4*(NBB+1)-4
      IF(IOPT.EQ.1.AND.JOPT.EQ.1) N1=N2
      DO 85 I=1,NS
      JX(I)=N2*I-1
   85 IF(IOPT.EQ.0) JX(I)=N1+N2*I-1
      IF(.NOT.NOPT.EQ.1) GO TO 35
C  STATIC ANALYSIS IS PERFORMED NEXT
      DO 5 I=1,N
      DO 5 J=1,N
    5 YQ(I,J)=YK(I,J)
      CALL MATINV(N,0,DET)
      DO 6 I=1,N
      DO 6 J=1,N
    6 D(I)=D(I)+YQ(I,J)*P(J)
      WRITE(5,404)
      CALL OUTPUT2(N,1,N,1,1)
      CALL STRESS(1)
      IF(KL.EQ.0) WRITE(5,407)
      IF(.NOT.KL.EQ.0) WRITE(5,408)
      CALL OUTPUT1(NS,JX,STX)
      WRITE(5,406)
      CALL OUTPUT1(NS,JX,STY)
      IF(.NOT.KOPT.EQ.1) GO TO 120
C  DYNAMIC  RESPONSE ANALYSIS
   35 CM=FFIN(3)
      CS=FFIN(3)
      NO=FFIN(3)
      T1=FFIN(3)
      DO 30 I=1,NO
   30 OM(I)=6.28318*FFIN(3)
      IM=FFIN(3)
      ND=FFIN(3)
      INI=FFIN(3)
      MI=FFIN(3)
      IF(ND.EQ.0) GO TO 108
      NI=FFIN(3)
```

```
      PF(1)=FFIN(3)
C  CM, CS DAMPING RATIOS FOR MATERIAL AND/OR SLIP DAMPING
C  NO = NUMBER OF FREQUENCIES IN OM, T1 = TIME INTERVAL
C  OM = MODAL FREQUENCIES, IM = MODE OF FREQUENCY USED IN
C  DAMPING, ND = DISPL. NO. AT LOAD APPLICATION, INI=0 IS OPTION
C  IN CASE OF NO INITIAL DISPL., MI = NO. OF T1, PF(I) = LOADS
C  AT BEGINING OF EACH T1, NI = NO. OF PF(I) IN INPUT
      NII=NI+1
C  LINEAR INTERPOLATION FOR SEGMENTS T1=.025 OF LOADING FUNCTION
      JD=.025/T1
      DO 102 I=2,NII
      PF(I)=FFIN(3)
      DIF=(PF(I)-PF(I-1))*T1/.025
      DO 102 J=1,JD
      K=(I-2)*JD+J
      XJ=J
  102 PT(K)=PF(I-1)+XJ*DIF
  108 CM=2.*CM*OM(IM)
      CS=2.*CS*OM(IM)
      DO 107 I=1,N
      P(I)=0.
  107 IF(INI.EQ.0) D(I)=0.
      IF(.NOT.ND.EQ.0) P(ND)=PT(1)
      WRITE(5,411)
      IF(.NOT.ND.EQ.0) WRITE(5,410) ND
      IF(.NOT.INI.EQ.0) WRITE(5,412)
      CALL OUTPUT2(N,0,NS,0,0)
C  P(I), D(I) ARE INITIAL LOAD AND/OR DISPLACEMENT VECTORS
      CALL NUMINT(ND,MI,N,NS,T1,IK,CM,CS,KL,INI)
      WRITE(5,408)
      IF(KL.EQ.0) WRITE(5,407)
      CALL OUTPUT1(NS,JX,STX)
      WRITE(5,406)
      CALL OUTPUT1(NS,JX,STY)
  120 CONTINUE
      END

      SUBROUTINE STRESS(KOPT)
      COMMON/DATA/EL,ET,A,B,H1,IOPT,JOPT,N1,N2,NBB,PTL,PLT,NS,KL
      COMMON A1(60,60),A2(60,60),A3(60,60),A5(700),D(60),
     1IA6(30),JX(20),A7(60),ST(20),EX(20),STX(20),STY(20)
      IF(.NOT.KL.EQ.0) GO TO 12
      DO 18 I=1,NS
   18 EX(I)=0.
   12 Y=1.
      IF(KL.EQ.0) Y=0.
      X=0.
      IF(KL.EQ.0) X=1.
      DO 10 I=1,NS
      IF(KOPT.GT.1) GO TO 15
      STX(I)=0.
      STY(I)=0.
   15 J=JX(I)
      J4=IABS(J-4)
      WI=D(J4)
      IF(NBB.LE.1) WI=0.
      WXX=(6.*(WI-D(J))+2.*A*D(J-2))/(A*A)
      Z=0.
      ZT=2.
      ZFR=0.
      ZBR=0.
      ZF=0.
      ZB=0.
      JB=IABS(J-N2)
      JF=J+N2
      JFR=J+2+N1
      JBR=J+2-N2
      IT=NS-I
      IF(IOPT.EQ.1.AND.I.EQ.1) GO TO 65
      IF(JOPT.EQ.1.AND.IT.EQ.0) GO TO 66
      Z=1.
      ZT=1.
   66 ZBR=1.
   65 ZFR=1.
      IF(JOPT.EQ.1.AND.IT.EQ.0) ZFR=0.
      ZR=0.
      IF(IOPT.EQ.0.AND.I.EQ.1) GO TO 67
      JBR=IABS(J+1-N2)
      ZB=1.
      ZR=1.
   67 IF(JOPT.EQ.0.AND.IT.EQ.0) GO TO 68
      JFR=J+N2+1
      ZF=1.
      ZR=1.
   68 WYY=ZT*(3.*(ZF*ZFR*D(JF)-(1.+Z*ZR)*D(J)+ZB*ZBR*D(JB))-
     1B*(ZFR*D(JFR)+2.*(1.+Z)*D(J+1)+ZBR*D(JBR)))/(B*B)
      K=J/N2+1
      STY1I=EL*(H1*WYY+PTL*(H1+EX(K))*WXX)+Y
      STYI=EL*(PTL*(Y*EX(K)-H1)*WXX-H1*WYY)
      TS=ABS(STY1I)-ABS(STYI)
      IF(TS.GE.0) STYI=STY1I
      TY=ABS(STYI)-ABS(STY(I))
      IF(TY.GE.0) STY(I)=STYI
      IF(KL.EQ.0) STXI=ET*H1*(PLT*WYY+WXX)
      IF(.NOT.KL.EQ.0) STXI=(-1.)*WXX*ST(K)
      TX=ABS(STXI)-ABS(STX(I))
   10 IF(TX.GE.0) STX(I)=STXI
      RETURN
      END

      SUBROUTINE OUTPUT1 (N,NX,XN)
      DIMENSION NX(20), XN(20)
  410 FORMAT(1X,'S',2X,5E13.5)
  411 FORMAT(1X,'ND',I8,4I13)
      J=1
      K=5
      IF(N.LT.5) K=N
   27 WRITE(5,411)(NX(I),I=J,K)
      WRITE(5,410)(XN(I),I=J,K)
      J=K+1
      K=J+4
      M=N-J
      IF(M.LT.4) K=N
      IF(J.LE.N) GO TO 27
      RETURN
      END

      SUBROUTINE OUTPUT2(N,IN,NS,TIME,LO)
      COMMON A1(60,60),A2(60,60),A3(60,60),A5(700),D(60),
     1IA6(30),NDT(20),A7(60),A9(20),B1(20),B2(20),B3(20)
      DIMENSION DT(20)
  450 FORMAT(1X/1X,'TIME=',F8.5,1X,'SECONDS',5X,'INTERVAL NO.',I4)
  452 FORMAT(1X/1X,'DISP.NOS.',15,4I12)
  454 FORMAT(1X,'DISPL.',2X,5E12.4)
      IF(LO.EQ.1) GO TO 460
      WRITE(5,450) TIME, IN
      DO 458 I=1,NS
      IJ=NDT(I)
  458 DT(I)=D(IJ)
  460 J=1
      K=5
      IF(NS.LT.7) K=NS
  456 IF (LO.EQ.1) GO TO 462
      WRITE(5,452)(NDT(I),I=J,K)
      WRITE(5,454)(DT(I),I=J,K)
      GO TO 464
  462 WRITE(5,452)(I,I=J,K)
      WRITE(5,454)(D(I),I=J,K)
  464 J=K+1
      K=J+4
      M=NS-J
      IF(M.LE.4) K=NS
```

```
      IF(J.LE.NS) GO TO 456
      RETURN
      END

      SUBROUTINE NUMINT(ND,NI,N,NS,T1,IK,CM,CS,KL,INI)
C  THIS ROUTINE NUMERICALLY INTEGRATES EQUATIONS OF MOTION
      COMMON YQ(60,60),YK(60,60),YM(60,60),PT(700),D(60),
     1IX(30),IA5(20),P(60),ST(20),EX(20),STX(20),STY(20)
      DIMENSION W1(60),W2(60),XA(60),XB(60)
      DO 109 I=1,N
      XA(I)=P(I)
      DO 109 J=1,N
  109 XA(I)=XA(I)-YK(I,J)*D(J)
      DO 100 I=1,N
      DO 100 J=1,N
  100 YQ(I,J)=YM(I,J)
      CALL MATINV(N,0,DET)
      DO 111 I=1,N
      DO 111 J=1,N
  111 W2(I)=W2(I)+YQ(I,J)*XA(J)
      T2=T1/2.
      T3=T1*T1/6.
      TIME=0.
      IN=0
      DO 197 I=1,N
      DO 197 J=1,N
  197 YQ(I,J)=CM*YM(I,J)
      IF(KL.EQ.0) GO TO 209
      DO 199 I=1,IK
      L=IX(I)
      DO 199 J=1,IK
      K=IX(J)
  199 YQ(L,K)=(1.+CS/CM)*YQ(L,K)
  209 DO 127 I=1,N
      DO 127 J=1,N
      AQ=YM(I,J)
      YM(I,J)=YQ(I,J)
  127 YQ(I,J)=AQ+T2*YM(I,J)+T3*YK(I,J)
      CALL MATINV(N,0,DET)
  115 IN=IN+1
      TIME=TIME+T1
      IF(.NOT.ND.EQ.0) P(ND)=PT(IN+1)
      DO 201 I=1,N
      IF(IN.GT.1) GO TO 117
      XA(I)=T2*W2(I)
      XB(I)=D(I)+2.*T3*W2(I)
      GO TO 201
  117 XA(I)=XA(I)+T1*W2(I)
      XB(I)=XB(I)+T1*XA(I)
  201 CONTINUE
      DO 203 I=1,N
      W1(I)=P(I)
      DO 203 J=1,N
  203 W1(I)=W1(I)-YM(I,J)*XA(J)-YK(I,J)*XB(J)
      DO 205 I=1,N
      W2(I)=0.
      DO 205 J=1,N
  205 W2(I)=W2(I)+YQ(I,J)*W1(J)
      DO 207 I=1,N
      D(I)=XB(I)+T3*W2(I)
  207 W1(I)=XA(I)+T2*W2(I)
C  PRINT DEFLECTIONS EVERY 8TH LOOP
      KN=KN+1
      IF(.NOT.KN.EQ.8) GO TO 211
      CALL OUTPUT2(N,IN,NS,TIME,0)
      KN=0
  211 CALL STRESS(IN)
      IF(IN.LT.NI) GO TO 115
      RETURN
      END
```

```
C  MATRIX INVERSION SUBROUTINE
      SUBROUTINE MATINV(N,M,DETERM)
      COMMON A(60,60),A1(60,60),A2(60,60),A5(700),A4(60),
     1IA6(30),IA7(20),A8(60),A9(20),B1(20),B2(20),B3(20)
      DIMENSION B(60,1), IPIVOT(60), INDEX(60,2), PIVOT(60)
      DETERM=1.0
      DO 20 J=1,N
   20 IPIVOT(J)=0
      DO 550 I=1,N
      AMAX=0.0
      DO 105 J=1,N
      IF (IPIVOT(J)-1) 60, 105, 60
   60 DO 100 K=1,N
      IF (IPIVOT(K)-1) 80, 100, 740
   80 IF (ABSF(AMAX)-ABSF(A(J,K))) 85, 100, 100
   85 IROW=J
      ICOLUM=K
      AMAX=A(J,K)
  100 CONTINUE
  105 CONTINUE
      IPIVOT(ICOLUM)=IPIVOT(ICOLUM)+1
      IF (IROW-ICOLUM) 140, 260, 140
  140 DETERM=-DETERM
      DO 200 L=1,N
      SWAP=A(IROW,L)
      A(IROW,L)=A(ICOLUM,L)
  200 A(ICOLUM,L)=SWAP
      IF(M) 260, 260, 210
  210 DO 250 L=1, M
      SWAP=B(IROW,L)
      B(IROW,L)=B(ICOLUM,L)
  250 B(ICOLUM,L)=SWAP
  260 INDEX(I,1)=IROW
      INDEX(I,2)=ICOLUM
      PIVOT(I)=A(ICOLUM,ICOLUM)
      DETERM=DETERM*PIVOT(I)
      A(ICOLUM,ICOLUM)=1.0
      DO 350 L=1,N
  350 A(ICOLUM,L)=A(ICOLUM,L)/PIVOT(I)
      IF(M) 380, 380, 360
  360 DO 370 L=1,M
  370 B(ICOLUM,L)=B(ICOLUM,L)/PIVOT(I)
  380 DO 550 L1=1,N
      IF(L1-ICOLUM) 400, 550, 400
  400 T=A(L1,ICOLUM)
      A(L1,ICOLUM)=0.0
      DO 450 L=1,N
  450 A(L1,L)=A(L1,L)-A(ICOLUM,L)*T
      IF(M) 550, 550, 460
  460 DO 500 L=1,M
  500 B(L1,L)=B(L1,L)-B(ICOLUM,L)*T
  550 CONTINUE
      DO 710 I=1,N
      L=N+1-I
      IF (INDEX(L,1)-INDEX(L,2)) 630, 710, 630
  630 JROW=INDEX(L,1)
      JCOLUM=INDEX(L,2)
      DO 705 K=1,N
      SWAP=A(K,JROW)
      A(K,JROW)=A(K,JCOLUM)
      A(K,JCOLUM)=SWAP
  705 CONTINUE
  710 CONTINUE
  740 RETURN
      END
```

```
      PROGRAM EIGENV
      REAL LAMBDA
      DIMENSION VALU(16),X(62),TITLE(13)
      COMMON D1(62,16),D2(62,16),VECO(16,62),AA(62),BB(62),EPSI(16),
     1D7(16),D8(16),D9(62)
  301 FORMAT (16I5)
  302 FORMAT (6E10.4)
  303 FORMAT(1X,6E11.4)
  304 FORMAT (I1)
  305 FORMAT (1X,15HEIGENVALUES ARE)
  306 FORMAT (1X,15HEIGENVECTOR NO.,I4,5X,12HFOR LAMBDA =,E15.7)
  307 FORMAT (13A6)
  308 FORMAT (1X,13A6)
  311 FORMAT (1X,34HCHECK K*X COMPARED WITH LAMBDA*M*X)
  312 FORMAT (1X,12HFOR LAMBDA =,E11.4)
  313 FORMAT (1X,2(2E12.4,7X))
  318 FORMAT(14F5.2)
      READ(5,307) TITLE
      WRITE(6,308) TITLE
      READ(5,301)N,NVEC,ITRS,IPR,IKU
      IF (N.EQ.0) STOP
      READ(5,302)(EPSI(I),I=1,NVEC)
      READ(5,304) IOPT
      IF (IOPT .EQ. 0) GO TO 100
      IF (IOPT .EQ. 1) GO TO 120
      STOP
  100 DO 105 I = 1,NVEC
  105 READ(5,318)(VECO(I,J),J=1,N)
      GO TO 150
  120 DO 130 I=1,NVEC
      DO 125 J=1,N
      VECO(I,J) = 0.0
      IF(I .EQ. J) VECO(I,J) = 1.0
  125 CONTINUE
  130 CONTINUE
  150 CALL FBMIN2(N,NVEC,VALU,ITRS,IPR,IKU)
      WRITE(6,305)
      WRITE(6,303)(VALU(I),I=1,NVEC)
      DO 40 I = 1,NVEC
      SUM = 0.0
      DO 32 J = 1,N
      IF (ABS(VECO(I,J)).GT.ABS(SUM)) SUM = VECO(I,J)
   32 CONTINUE
      SUM = 1.0/SUM
      DO 35 J = 1,N
   35 VECO(I,J) = VECO(I,J)*SUM
      WRITE(6,306) I,VALU(I)
      WRITE(6,303) (VECO(I,J),J=1,N)
   40 CONTINUE
      WRITE(6,311)
      DO 250 IVEC = 1,NVEC
      LAMBDA = VALU(IVEC)
      WRITE(6,312) LAMBDA
      DO 240 I = 1,N
      X(I) = VECO(IVEC,I)
  240 CONTINUE
      CALL KXMX (X,N)
      DO 245 I = 1,N
  245 BB(I) = BB(I)*LAMBDA
      WRITE(6,313) (AA(I),BB(I),I=1,N)
  250 CONTINUE
      END

      SUBROUTINE KXMX (X,N)
      REAL K,M
      DOUBLE PRECISION SUM1,SUM2
      DIMENSION X(62),K(62,62),M(62,62)
      COMMON D1(62,16),D2(62,16),D3(16,62),AA(62),BB(62),D6(16),D7(16),
     1D8(16),D9(62)
      COMMON/DATA/INDEX
      DATA(INDEX=1)
  301 FORMAT (1X,6E11.4)
      IF (INDEX.EQ.0) GO TO 10
      INDEX = 0
      DO 401 I=1,N
  401 READ(7,301)(K(I,J),J=1,N)
      DO 402 I=1,N
  402 READ(7,301)(M(I,J),J=1,N)
   10 DO 100 I = 1,N
      SUM1 = 0.0
      SUM2 = 0.0
      DO 90 J = 1,N
      SUM1 = SUM1 + K(I,J)*X(J)
      SUM2 = SUM2 + M(I,J)*X(J)
   90 CONTINUE
      AA(I) = SUM1
      BB(I) = SUM2
  100 CONTINUE
      RETURN
      END

      SUBROUTINE FBMIN2(NDFS,NVEC,VALU,ITRS,IPR,IKU)
      REAL NUMER1,NUMER2,NUM,NP,NNNP,NNNNP,NUMER
      DOUBLE PRECISION NUMER,DENOM
      DIMENSION P(62),VALU(16),VV(62),X(62),G(62),S(62),XEM(62),
     1GXEM(62),XNN(16,16)
      COMMON BXX(62,16),BX(62,16),VECO(16,62),AA(62),BB(62),EPSI(16),
     1NP(16),NNNP(16),NNNNP(62)
   27 FORMAT(1X,'KVEC',2X,'MIN',2X,'ITER',6X,'FXEM',10X,'DEL',12X,'TEST'
     110X,'ALPHA',5X,'LOOP')
   28 FORMAT (I4,I5,I7,E15.8,E12.4,E16.4,E14.4,I6)
      NUMER = 0.0
      DENOM = 0.0
      DO 503 I = 1,NDFS
      VV(I) = 0.0
      DO 503 J = 1,NVEC
  503 BX(I,J) = 0.0
      ITND=2*NDFS
      KVEC=1
      DO 449 I=1,NDFS
  449 X(I)=VECO(KVEC,I)
      XX = 0.0
      MIN = 0
      DO 10 I = 1,NDFS
      IF (ABS(X(I)).LT.XX) GO TO 10
      MIN = I
      XX = ABS(X(I))
   10 CONTINUE
      MINO = MIN
      DO 447 I=1,NDFS
  447 X(I)=X(I)/XX
   49 ITER=0
      IR = 0
  350 CALL FANDG(X,1,F1,G,MIN,MINO,ITER,NUMER,DENOM,NDFS,KVEC,NVEC)
      IF (IPR.NE.0) WRITE(6,27)
      F3 = F1
      NUMER1=NUMER
      DENOM1=DENOM
      IF (KVEC .NE. NDFS) GO TO 85
      VALU(KVEC)=F1
      DO 67 I=1,NDFS
   67 VECO(KVEC,I)=X(I)
      GO TO 69
   85 DO 50 I=1,NDFS
   50 S(I)=-G(I)
      ITER=1
  200 CALL FANDG(S,0,F,G,MIN,MINO,ITER,NUMER,DENOM,NDFS,KVEC,NVEC)
      NUMER2=NUMER
      DENOM2=DENOM
      NUM=0.0
      DEN=0.0
      DO 51 I=1,NDFS
```

```
      NUM=NUM+X(I)*AA(I)
   51 DEN=DEN+X(I)*BB(I)
      U=(NUMER2*DEN)-(NUM*DENOM2)
      V=(NUMER2*DENOM1)-(NUMER1*DENOM2)
      W=(NUM*DENOM1)-(NUMER1*DEN)
      V=V/U
      W=W/U
      U=1.0
      TS1=-V/(2.0*U)
      TS2 = SQRT(V**2 - 4.0*U*W)/(2.0*U)
      TS3=-TS2
      ALPHA1=TS1+TS2
      ALPHA2=TS1+TS3
      IF (ALPHA1 .LT. 0.0 .AND. ALPHA2 .LT. 0.0) GO TO 76
      IF (ALPHA1 .GT. 0.0 .AND. ALPHA2 .GT. 0.0) GO TO 60
      ALPHA=AMAX1(ALPHA1,ALPHA2)
      GO TO 71
   60 ALPHA=AMIN1(ALPHA1,ALPHA2)
      GO TO 71
   76 DO 79 I=1,NDFS
   79 XEM(I)=X(I)+ALPHA1*S(I)
      CALL FANDG(XEM,0,F1,G,MIN,MINO,ITER,NUMER,DENOM,NDFS,KVEC,NVEC)
      DO 80 I=1,NDFS
   80 XEM(I)=X(I)+ALPHA2*S(I)
      CALL FANDG(XEM,0,F2,G,MIN,MINO,ITER,NUMER,DENOM,NDFS,KVEC,NVEC)
      IF (F1 .LT. F2) GO TO 77
      ALPHA=ALPHA2
      GO TO 78
   77 ALPHA=ALPHA1
   78 DO 81 I=1,NDFS
   81 XEM(I)=X(I)+ALPHA*S(I)
      DO 82 I=1,NDFS
   82 X(I)=XEM(I)
      GO TO 350
   71 TA=0.0
      DO 52 I=1,NDFS
      TA=TA+G(I)*G(I)
   52 XEM(I)=X(I)+ALPHA*S(I)
      RMAX=0.0
      IMAX=0
      DO 451 I=1,NDFS
      IF ((ABS(XEM(I))) .LE. RMAX) GO TO 451
      RMAX=ABS(XEM(I))
      IMAX=I
  451 CONTINUE
      IF (RMAX .LE. 5.0) GO TO 454
      MINO=MIN
      MIN=IMAX
      DO 452 I=1,NDFS
  452 X(I)=XEM(I)
      XX=X(MIN)
      DO 450 I=1,NDFS
  450 X(I)=X(I)/XX
      GO TO 49
  454 CALL FANDG (XEM,1,FXEM,GXEM,MIN,MINO,ITER,NUMER,DENOM,NDF5
     1,KVEC,NVEC)
      NUMER1=NUMER
      DENOM1=DENOM
      GS=0.0
      AG=0.0
      BE=0.0
      DO 53 I=1,NDFS
      GS=GS+S(I)*GXEM(I)
      AG=AG+S(I)*S(I)
   53 BE=BE+GXEM(I)*GXEM(I)
      BETA=BE/TA
      AG=SQRT(AG)
      BE=SQRT(BE)
      TEST=GS/(AG*BE)
      IF (ABS(TEST).GT.1.0E-3) GO TO 320
  319 LOOP = 0
      DO 54 I=1,NDFS
   54 S(I)=-GXEM(I)+BETA*S(I)
      DIF = F3 - FXEM
      DEL = DIF
      CONTINUE
      IF (IPR.NE.0) WRITE(6,28) KVEC,MIN,ITER,FXEM,DEL,TEST,ALPHA
      IF (DEL.LT.0.0) GO TO 370
      NEG = 0
      DO 360 I = 1,NDFS
      G(I) = GXEM(I)
  360 X(I) = XEM(I)
      IF (ABS(DIF/FXEM).LT.EPSI(KVEC)) GO TO 400
      F3 = FXEM
      ITER=ITER+1
      IF (ITER.GT.ITND) GO TO 49
      IF (IR.EQ.0 .AND. ITER.EQ.ITRS) GO TO 300
      GO TO 200
  320 CONTINUE
      IF (IPR.NE.0) WRITE(6,28) KVEC,MIN,ITER,FXEM,DEL,TEST,ALPHA,LOOP
      IF (KVEC.EQ.NDFS-1) GO TO 319
      LOOP = LOOP + 1
      IF (LOOP.GT.20) GO TO 355
      IF (LOOP.EQ.1) GO TO 340
      IF ((TEST*TESTL).GT.0.0) GO TO 335
      TSTA = ALPHAL + SIGN*(ALPHAL-ALPHA)*GSL/(GSL-GS)
      TINC = 0.6*TINC
  345 ALPHAL = ALPHA
      ALPHA = TSTA
      GSL = GS
      TESTL = TEST
      SIGN = 1.0
      IF (TEST.GT.0.0) SIGN = -1.0
      DO 347 I = 1,NDFS
  347 XEM(I) = X(I) + ALPHA*S(I)
      GO TO 454
  335 CONTINUE
      TSTA = ALPHA + SIGN*TINC
      GO TO 345
  340 TINC = 0.1*ALPHA
      SIGN = 1.0
      IF (TEST.GT.0.0) SIGN = -1.0
      GO TO 335
  355 GO TO 319
  300 CONTINUE
      IR = 1
      GO TO 49
  370 CONTINUE
      NEG = NEG + 1
      IF (NEG.EQ.1) GO TO 49
      FXEM = F3
  400 CONTINUE
      VALU(KVEC)=FXEM
  301 FORMAT (15H0EIGENVALUE NO.,I5,5X,1H=,E15.7,5X,14HEIGENVECTOR IS)
  302 FORMAT (10E13.6)
      IF(IKU.NE.0) WRITE(6,301) KVEC,FXEM
      SUM1 = 0.0
      DO 303 I = 1,NDFS
  303 SUM1 = SUM1 + XEM(I)**2
      SUM1 = 1.0/SQRT(SUM1)
      DO 304 I = 1,NDFS
  304 X(I) = XEM(I)*SUM1
      IF(IKU.NE.0) WRITE(6,302) (X(I),I=1,NDFS)
      DO 401 I=1, NDFS
  401 VECO(KVEC,I)=XEM(I)
      IF (KVEC .EQ. NVEC) GO TO 69
      KVEC=KVEC+1
      CALL KXMX (XEM,NDFS)
      BBNORM = 0.0
      DO 402 I = 1,NDFS
  402 BBNORM = BBNORM + BB(I)**2
      BBNORM = SQRT (BBNORM)
```

```
      DO 403 I = 1,NDFS
  403 BB(I) = BB(I)/BBNORM
      JJ=KVEC-1
      DO 58 I=1,NDFS
   58 BX(I,JJ)=BB(I)
      DO 40 I=1,NDFS
   40 P(I)=VECO(KVEC,I)
      IF (KVEC .GT. 2) GO TO 57
      DEN1=0.0
      DO 64 I=1,NDFS
   64 DEN1=DEN1+P(I)*BX(I,1)
      DO 65 I=1,NDFS
   65 X(I)=P(I)-DEN1*BX(I,1)
      GO TO 92
   57 IF (KVEC .GT. 3) GO TO 229
      DEN1=0.0
      DO 59 I=1,NDFS
   59 DEN1=DEN1+BX(I,1)*BX(I,2)
      RAS=(1.0-(DEN1)**2)
      DO 505 I = 1,NVEC
      DO 505 J = 1,NVEC
  505 XNN(I,J) = 0.0
      XNN(1,1)=1.0/RAS
      XNN(1,2)=-DEN1/RAS
      XNN(2,1)=-DEN1/RAS
      XNN(2,2)=1.0/RAS
      GO TO 72
  229 KVEC=KVEC-1
      DO 603 I=1,NDFS
      DO 603 J=1,NVEC
  603 BXX(I,J)=BX(I,J)
      CALL INGEN(XNN,NDFS,KVEC)
      KVEC=KVEC+1
   72 DO 604 I=1,NDFS
      DO 604 J=1,NVEC
  604 BXX(I,J)=BX(I,J)
      CALL PROD(P,XNN,NDFS,KVEC)
      DO 61 I=1,NDFS
   61 X(I)=P(I)-NNNNP(I)
   92 CONTINUE
      XX = 0.0
      IMAX = 0
      DO 506 I = 1,NDFS
      IF (ABS(X(I)).LT.XX) GO TO 506
      XX = ABS(X(I))
      IMAX = I
  506 CONTINUE
      DO 507 I = 1,NDFS
  507 X(I) = X(I)/XX
      IF (MIN.EQ.IMAX) GO TO 49
      MINO = MIN
      MIN = IMAX
      GO TO 49
   69 RETURN
      END

      SUBROUTINE FANDG(X,LFG,F,G,MIN,MINO,ITER,NUMER,DENOM,NDFS
     1,KVEC,NVEC)
      REAL N,NN,NG,NNNG,NNNNG,NUMER
      DOUBLE PRECISION NUMER,DENOM
      DIMENSION X(62),G(62),NN(16,16)
      COMMON N(62,16),BX(62,16),D3(16,62),AA(62),BB(62),D6(16),
     1NG(16),NNNG(16),NNNNG(62)
      CALL KXMX(X,NDFS)
      NUMER = 0.0
      DENOM = 0.0
      DO 22 I=1,NDFS
      NUMER=NUMER+X(I)*AA(I)
   22 DENOM=DENOM+X(I)*BB(I)
C     CALCULATE FUNCTION VALUE
      F=NUMER/DENOM
      IF(LFG .EQ. 0) GO TO 24
C     CALCULATE GRADIENT
      TSTA = 2.0/DENOM
      DO 23 I=1,NDFS
   23 G(I) = TSTA*(AA(I)-F*BB(I))
      IF (KVEC .EQ. 1) GO TO 38
      IF (MIN .NE. MINO) GO TO 40
      N(MIN,1)=1.0
      DO 25 I=1,NDFS
   25 N(I,2)=BX(I,1)
      IF (ITER .GE. 1) GO TO 11
      IF (KVEC .GT. 2) GO TO 12
      DO 504 I = 1,NDFS
  504 N(I,1) = 0.0
      N(MIN,1) = 1.0
      XXX=BX(MIN,1)
      RAS=(1.0-(XXX)**2)
      NN(1,1)=1.0/RAS
      NN(1,2)=-XXX/RAS
      NN(2,1)=-XXX/RAS
      NN(2,2)=1.0/RAS
      GO TO 11
   40 IF (ITER .GE. 1) GO TO 11
      DO 56 I=1,NDFS
      DO 56 J=1,NVEC
   56 N(I,J)=0.0
      DO 57 I=1,NVEC
      DO 57 J=1,NVEC
   57 NN(I,J)=0.0
      N(MIN,1)=1.0
      DO 35 I=1,NDFS
   35 N(I,2)=BX(I,1)
      XXX=BX(MIN,1)
      RAS=(1.0-(XXX)**2)
      NN(1,1)=1.0/RAS
      NN(1,2)=-XXX/RAS
      NN(2,1)=-XXX/RAS
      NN(2,2)=1.0/RAS
      IF (KVEC .EQ. 2) GO TO 11
      LL=KVEC-1
      DO 31 IV = 2,LL
      DO 32 I=1,NDFS
   32 BB(I) = BX(I,IV)
      KVEC = IV + 1
      CALL INGEN (NN,NDFS,KVEC)
      KVEC = IV
      K = KVEC + 1
      DO 33 I=1,NDFS
   33 N(I,K) = BX(I,KVEC)
   31 CONTINUE
      KVEC = KVEC + 1
      GO TO 11
   12 JJ=KVEC-1
      DO 26 I=1,NDFS
   26 BB(I)=BX(I,JJ)
      CALL INGEN(NN,NDFS,KVEC)
      DO 27 I=1,NDFS
   27 N(I,KVEC)=BX(I,JJ)
   11 CALL PROD(G,NN,NDFS,KVEC)
      DO 37 I=1,NDFS
   37 G(I)=G(I)-NNNNG(I)
   38 G(MIN)=0.0
   24 RETURN
      END

      SUBROUTINE PROD(G,NN,NDFS,KVEC)
      REAL N,NN,NG,NNNG,NNNNG
      DIMENSION G(62),NN(16,16)
      COMMON N(62,16),D2(62,16),D3(16,62),D4(62),X(62),D6(16),
     1NG(16),NNNG(16),NNNNG(62)
      DO 31 I=1,KVEC
```

```
      SUM=0.0
      DO 32 J=1,NDFS
   32 SUM=SUM+N(J,I)*G(J)
      NG(I)=SUM
   31 CONTINUE
      DO 33 I=1,KVEC
      SUM=0.0
      DO 34 J=1,KVEC
   34 SUM=SUM+NN(I,J)*NG(J)
      NNNG(I)=SUM
   33 CONTINUE
      DO 35 I=1,NDFS
      SUM=0.0
      DO 36 J=1,KVEC
   36 SUM=SUM+N(I,J)*NNNG(J)
      NNNNG(I)=SUM
   35 CONTINUE
      RETURN
      END

      SUBROUTINE INGEN(NN,NDFS,KVEC)
      REAL NN,N,NG,NNNG,NNNNG
      DIMENSION PN(62),TM(16,16),A1(16,16),A2(16),NN(16,16)
      COMMON N(62,16),D2(62,16),D3(16,62),D4(62),X(62),D6(16),
     1NG(16),NNNG(16),NNNNG(62)
      CALL PROD(X,NN,NDFS,KVEC)
      DO 10 I=1,NDFS
   10 PN(I)=X(I)-NNNNG(I)
      A0=0.0
      DO 11 I=1,NDFS
   11 A0=A0+PN(I)*PN(I)
      A0=1.0/A0
      KKK=KVEC-1
      DO 12 I=1,KKK
      DO 13 J=1,KKK
   13 TM(I,J)=NNNG(I)*NNNG(J)
   12 CONTINUE
      DO 14 I=1,KKK
      DO 15 J=1,KKK
   15 A1(I,J)=NN(I,J)+A0*TM(I,J)
   14 CONTINUE
      DO 16 I=1,KKK
   16 A2(I)=-A0*NNNG(I)
      DO 17 I=1,KKK
      DO 17 J=1,KKK
   17 NN(I,J)=A1(I,J)
      JJ=KVEC
      DO 18 I=1,KKK
      NN(JJ,I)=A2(I)
   18 NN(I,JJ)=A2(I)
      NN(JJ,JJ)=A0
      RETURN
      END
```